Rat Polymerase β Binds Double-Stranded DNA Using Exclusively the 8-kDa Domain. Stoichiometries, Intrinsic Affinities, and Cooperativities[†,‡]

Maria J. Jezewska, Roberto Galletto, and Wlodzimierz Bujalowski*

Department of Human Biological Chemistry and Genetics and the Sealy Center for Structural Biology, The University of Texas Medical Branch at Galveston, 301 University Boulevard, Galveston, Texas 77555-1053

Received February 21, 2003; Revised Manuscript Received March 20, 2003

ABSTRACT: Analyses of the interactions of rat polymerase β (rat pol β) with a double-stranded DNA have been performed using the quantitative fluorescence titration and fluorescence energy transfer techniques. The obtained results show that rat pol β binds to dsDNA oligomers with the site-size of the enzyme−dsDNA complex $n = 5 \pm 1$ base pairs. The small site-size of the complex is a consequence of engagement of only the 8-kDa domain in intrinsic interactions with the dsDNA. This conclusion is directly supported by the fluorescence energy transfer between the single tryptophan residue on the 31-kDa domain and fluorescence acceptor located on the DNA. The dsDNA oligomer is bound at a distance of at least 55 Å from the tryptophan, excluding the 31-kDa domain from any closed contact with the DNA. Moreover, in the complex with the dsDNA, the enzyme is bound in "open" conformational state. The intrinsic interactions are accompanied by a net release of about four to five ions. The net ion release is dominated by cations as a result of the exclusive engagement of the 8-kDa domain in interactions. Magnesium affects the net ion release through direct binding of Mg^{2+} cations to the protein. Surprisingly, binding of rat pol β to the dsDNA is characterized by strong positive cooperative interactions, a very different behavior from that previously observed for pol β complexes with the ssDNA and gapped DNAs. Contrary to intrinsic affinities, cooperative interactions are accompanied by a net uptake of about three to five ions. Anions have a large contribution to the net ion uptake, indicating that cooperative interactions characterize protein−protein interactions. The significance of these results for the pol β functioning in damaged-DNA recognition processes is discussed.

Polymerase β (pol β) plays a very specialized function in the mammalian cell DNA-repair machinery, which includes gap-filling synthesis in mismatch repair, repair of monofunctional adducts, UV-damaged DNA, and abasic lesions in DNA (*1*−*7*). A fundamental feature of the pol β functioning is that the enzyme must recognize a specific structure of the damaged DNA and the recognition process must precede the chemical step of the DNA synthesis. The complexity of the recognition process is reflected in the complexity of the total DNA-binding site of the polymerase. The enzyme possesses two structural domains: a large 31-kDa catalytic domain and a small 8-kDa domain (*7*). Similar structural arrangement has been indicated for several other DNA polymerases engaged in DNA repair, although their DNA binding properties have not yet been quantitatively examined (*8*−*11*). Both the 8- and 31-kDa domains have DNA-binding capability; thus, the total DNA-binding site is built of two DNA-binding subsites (*12*−*15*). However, only the DNA-binding subsite on the 8-kDa domain has been found to have similar and significant affinity for both ss and dsDNA (*16*, *17*). Moreover, the binding of Mg^{2+} cations to the 8-kDa domain specifically controls the site-size and the nucleic acid affinity of its DNA-binding subsite.

Quantitative thermodynamic analyses have shown a very complex DNA-binding mechanism of both human and rat pol β. The enzymes bind the ssDNA in two binding modes that differ in the number of occluded nucleotide residues: the $(\text{pol } \beta)_{16}$ and $(\text{pol } \beta)_5$ binding modes (*12*−*15*). The existence of the two binding modes is a result of spatial separation of the two DNA-binding subsites of the polymerase, located on two structurally different domains, with very different DNA binding capabilities (*7*, *12*−*15*). In the $(\text{pol } \beta)_{16}$ binding mode, both the 8- and the 31-kDa domains are involved in interactions with the ssDNA; i.e., the total DNA-binding site of the enzyme is engaged in the complex. In the $(\text{pol } \beta)_5$ binding mode, only the 8-kDa domain is engaged in interactions with the ssDNA (*12*−*15*).

The ability of the 8-kDa domain to interact with the ss and dsDNA is crucial for anchoring the enzyme to gapped-DNA substrates (*14*−*16*). The 8-kD domain binds to the ss and/or dsDNA part of the substrate downstream from the primer. The association of the 31-kDa domain of the enzyme with the dsDNA part of the gapped DNA substrate, containing the primer, follows this process. Kinetic studies of human and rat pol β interactions with the ssDNA, in the $(\text{pol } \beta)_{16}$ and $(\text{pol } \beta)_5$ binding modes, show that in both binding modes the formation of the complex is initiated through a very fast, diffusion-controlled association of the DNA-binding subsite located on the 8-kDa domain (*18*, *19*). Recent kinetic analyses of the gapped DNA recognition by human and rat

[†] This work was supported by NIH Grant GM-58675 (to W.B.).
[‡] Brookhaven Protein Data Bank deposition: 1BPD, 1BPY.
* To whom correspondence should be addressed. Phone: 409-772-5634. Fax: 409-772-1790. E-mail: wbujalow@utmb.edu.

10.1021/bi030046f CCC: $25.00
Published on Web 04/26/2003

pol β clearly indicate that the binding is also initiated through the 8-kDa domain (*20*).

One of the most puzzling questions for understanding the damaged DNA recognition by pol β is the following. How does the enzyme recognize the specific structure of the damaged DNA in the context of the overwhelming presence of the dsDNA? In other words, elucidation of the pol β interactions with the dsDNA is one of the fundamental steps toward understanding the molecular mechanism of the DNA recognition by the polymerase. Such analysis may also provide important insights about the recognition mechanisms of DNA substrates by other DNA repair polymerases. Despite its paramount importance for understanding the DNA recognition process, the direct analysis of pol β interactions with the dsDNA has not yet been quantitatively addressed.

In this communication, we report thermodynamic analyses of rat pol β interactions with the dsDNA. We provide direct evidence that the site-size of the enzyme−dsDNA complex is 5 ± 1 bases and the binding process is characterized by salt-controlled cooperative interactions. The enzyme binds the dsDNA exclusively through the 8-kDa domain in an open conformation. The 31-kDa domain is not engaged in interactions with the nucleic acid. The combined intrinsic and cooperative interactions result in affinity for the dsDNA that is significantly higher than the affinity for the ssDNA, excluding the possibility that the ssDNA plays a significant role in the initial stages of the gapped DNA recognition process. A plausible model for the role of strong cooperative interactions in the DNA substrate recognition by pol β is discussed.

MATERIALS AND METHODS

Reagents and Buffers. All solutions were made with distilled and deionized >18 MΩ (Milli-Q Plus) water. All chemicals were reagent grade. Buffer C is 10 mM sodium cacodylate adjusted to pH 7.0 with HCl, 0.1 mM EDTA, 1 mM DTT,[1] and 10% glycerol. Temperatures and concentrations of salts in the buffer are indicated in the text.

Rat Pol β. Rat polymerase β was purified, as previously described (*12*−*15*). The concentration of the protein was spectrophotometrically determined using the extinction coefficient $\epsilon_{280} = 2.1 \times 10^4\ cm^{-1}\ M^{-1}$ obtained by the method based on Edeldoch's approach (*12*, *21*, *22*).

Nucleic Acids. DNA oligomers were purchased from Midland Certified Reagents (Midland, Texas). Oligomers were at least >95% pure as judged by autoradiography on polyacrylamide gels. Labeled ssDNA oligomer contains a fluorescent label, 7-diethylamino-3-(4′-maleimidylphenyl)-4-methylcoumarin (CP) or 7-methoxycoumarin (CPM), attached to the 5′ or 3′ end through a six-carbon linker. Concentrations of all ssDNA oligomers have been spectrophotometrically determined as described previously by us (*23*−*25*). The dsDNA substrate was obtained by mixing the ssDNA oligomers at given concentrations, warming the mixture for 5 min at 95 °C and slowly cooling for a period of ∼3−4 h (*23*−*25*). The integrity of the dsDNA oligomers has been checked by UV melting and analytical ultracentrifugation techniques (*23*−*25*).

Fluorescence Measurements. Steady-state fluorescence titrations were performed using a SLM-AMINCO 8100 spectrofluorometer. To avoid possible artifacts due to the fluorescence anisotropy of the sample, polarizers were placed in excitation and emission channels and set at 90° and 55° (magic angle), respectively (*26*, *27*). Formation of the complex was followed by monitoring the fluorescence of the CP-labeled DNA ($\lambda_{ex} = 435$ nm; $\lambda_{em} = 480$ nm). Computer fits were performed using KaleidaGraph software (Synergy Software, PA) and Mathematica (Wolfram Research, IL). The relative fluorescence increase of the nucleic acid, ΔF, upon binding the polymerase is defined as $\Delta F = (F_i - F_0)/F_0$, where F_i is the fluorescence of the nucleic acid solution at a given titration point "*i*" and F_0 is the initial fluorescence of the sample.

Quantum Yield Determination. Fluorescence quantum yields of the rat pol β tryptophan and the fluorescent marker CPM attached to the dsDNA were determined by the comparative method of Parker and Reese, using quinine bisulfate in 0.1 N H_2SO_4 as a reference (absolute quantum yield $q_R = 0.7$) (*28*−*30*).

Determination of the Average Fluorescence Energy Transfer Efficiency from the Donor, Tryptophan Residue on the 31-kDa Domain, to an Acceptor, CPM, Located on the dsDNA. The true Förster efficiency of the fluorescence energy transfer, E, from the donor, a single tryptophan residue located on the 31-kDa domain of rat pol β, to the acceptor, the CPM residue located at the 5′ or 3′ end of a dsDNA oligomerm, has been determined using two apparent fluorescence energy transfer efficiencies. The energy transfer efficiency, E_D, obtained from the quenching of the donor fluorescence is defined for the examined pol β−dsDNA oligomer system by (*21*−*23*)

$$E_D = \left(\frac{1}{\nu_D}\right)\left(\frac{F_D - F_{DA}}{F_D}\right) \quad (1)$$

where F_D and F_{DA} are the fluorescence of the donor in the absence and presence of the acceptor, respectively, and ν_D is the fraction of the donor in the complex with the acceptor. The quantity ν_D is determined using binding parameters for a given DNA substrate obtained from the thermodynamic analysis of the enzyme−dsDNA interactions (see below).

The apparent fluorescence transfer efficiency, E_A, has been determined, using the sensitized acceptor fluorescence, by measuring the fluorescence intensity of the acceptor (CPM residue), excited at a wavelength where a donor (tryptophan) predominantly absorbs, in the absence and presence of the donor. The fluorescence intensities of the acceptor in the absence, F_A, and presence, F_{AD}, of the donor are defined as (*23*−*25*)

$$F_A = I_0 \epsilon C_{AT} \phi_F^A \quad (2a)$$

and

$$F_{AD} = (1 - \nu_A)F_A + I_0 \epsilon_A \nu_A C_{AT} \phi_B^A + I_0 \epsilon_D C_{DT} \nu_D \phi_B^A E_A \quad (2b)$$

where I_0 is the intensity of incident light, C_{AT} and C_{DT} are the total concentrations of acceptor and donor, ν_A is the

[1] Abbreviations: DTT, dithiothreitol; EDTA, ethylenediaminetetraacetic acid disodium salt; CP, 7-diethylamino-3-(4′-maleimidylphenyl)-4-methylcoumarin; CPM, 7-methoxycoumarin; MCT, macromolecular competition titration method.

fraction of acceptors in the complex with donors, ϵ_A and ϵ_D are the molar absorption coefficients of acceptor and donor at the excitation wavelength, respectively, ϕ_F^A and ϕ_B^A are the quantum yields of the free and bound acceptors, and E_A is the fluorescence energy transfer efficiency determined by the acceptor-sensitized emission. All quantities in eqs 2a and 2b can be experimentally determined. Dividing eq 2b by eq 2a and rearranging provides the fluorescence energy transfer efficiency, E_A, as

$$E_A = \left[\frac{1}{\nu_D}\right]\left(\frac{\epsilon_A C_{AT}}{\epsilon_D C_{DT}}\right)\left[\left(\frac{\phi_F^A}{\phi_B^A}\right)\left(\frac{F_{AD}}{F_A}\right) - 1\right] + \nu_A\left(\frac{\epsilon_A C_{AT}}{\epsilon_D C_{DT}}\right)\left[\left(\frac{\phi_F^A}{\phi_B^A}\right) - 1\right] \quad (3)$$

As we pointed out, the fluorescence energy transfer efficiencies, E_D and E_A, are apparent quantities. E_D is the fraction of the photons absent in the donor emission as a result of the presence of an acceptor, including transfer to the acceptor and possible nondipolar quenching processes, and E_A is a fraction of all photons absorbed by the donor that were transferred to the acceptor. The true Förster energy transfer efficiency, E, is the fraction of photons absorbed by the donor and transferred to the acceptor in the absence of any additional nondipolar quenching mechanisms (*27*). The value of E is related to the apparent quantities E_D and E_A by (*31*)

$$E = \frac{E_A}{1 - E_D + E_A} \quad (4)$$

Thus, measurements of the transfer efficiency, using both methods, are not alternatives but parts of the entire analysis used to obtain the true efficiency of the fluorescence energy transfer process, E.

The fluorescence energy transfer efficiency between the donor and acceptor dipoles, E, is related to the distance, R, separating the dipoles by (*27*)

$$R = R_0\left[\frac{(1 - E)}{E}\right]^{1/6} \quad (5)$$

and

$$R_0 = 9790(\kappa^2 n^{-4} \phi_d J)^{1/6} \quad (6)$$

where R_0 is the so-called Förster critical distance (Å), the distance at which the transfer efficiency is 50%, κ^2 is the orientation factor, ϕ_d is the donor quantum yield in the absence of the acceptor, and n is the refractive index of the medium ($n = 1.4$) (*27*). The overlap integral, J, characterizes the resonance between the donor and acceptor dipoles and has been evaluated by integration of the mutual area of overlap between the donor emission spectrum, $F(\lambda)$, and the acceptor absorption spectrum, $\epsilon_A(\lambda)$ (*27*).

The fluorescence transfer efficiency determined for a single donor−acceptor pair depends on the distance between the donor and the acceptor, R, and the factor κ^2, describing the mutual orientation of the donor and acceptor dipoles. The factor κ^2 can assume a value from 0 to 4. For complete random orientation of the acceptor and the donor, $\kappa^2 = 0.67$ (*27*). On the other hand, because the distance between a donor and an acceptor depends on $^1/_6$ the power of κ^2, only the two extreme values (0 or 4) resulting from a peculiar orientation of the donor and acceptor dipoles and complete dipole immobilization on the time scale of their fluorescence lifetimes would significantly affect the determined fluorescence energy transfer efficiencies and, in turn, conclusions about distances (*24*, *25*). The value of κ^2 cannot be directly experimentally determined. However, the effect of κ^2 can be experimentally assessed by examining either multiple donor−acceptor pairs or the same donor−acceptor pair in different orientations and environments (*32*). Very similar energy transfer efficiencies obtained in such experimental approaches effectively exclude unfavorable values of κ^2. Furthermore, the mobility of the donor and acceptor on the time scale of their fluorescence lifetimes can be estimated from the measured limiting anisotropies of the donor and acceptor (*23*−*25*, *32*).

Time-Dependent Fluorescence Measurements. Time-dependent fluorescence lifetime and anisotropy measurements have been performed using an IBH 5000U time-correlated single photon counting instrument (IBH, Glasgow, U.K.) equipped with polarizers as well as excitation and emission monochromators. The protein fluorescence has been excited at 295 nm using a coaxial nanosecond flash lamp, and emission was recorded at 345 nm (20 nm band-pass). Excitation of the CPM at 380 nm was performed with a nanosecond light emitting diode with emission recorded at 415 nm. At least 20 000 counts were collected at the peak with vertical orientation of both polarizers with respect to the direction of the light beam. Glycogen solution was used as a reference for the excitation source profile. Deconvolution analyses of total fluorescence emission and anisotropy decay curves were performed using the nonlinear least-squares software provided by the manufacturer.

Determination of Thermodynamically Rigorous Binding Isotherms of Rat Pol β−dsDNA Complexes. In this work, we followed the binding of rat pol β to the dsDNA oligomer by monitoring the fluorescence increase, ΔF_{obs}, of the coumarin-labeled nucleic acid upon formation of the complex. To obtain rigorous estimates of the average degree of binding, $\sum\Theta_i$ (number of bound protein molecules per dsDNA oligomer), and the free protein concentration, P_F, independently of any assumption about the relationship between the observed spectroscopic signal and $\sum\Theta_i$, we applied an approach previously described by us (*33*−*37*). Briefly, each different possible "i" complex of rat pol β with the dsDNA contributes to the experimentally observed fluorescence increase, ΔF_{obs}. Thus, ΔF_{obs} is functionally related to $\sum\Theta_i$ by

$$\Delta F_{obs} = \sum \Theta_i \Delta F_i \quad (7)$$

where ΔF_i is the molecular parameter characterizing the maximum fluorescence increase of the nucleic acid with rat pol β bound in complex "i". The same value of ΔF_{obs}, obtained at two different total nucleic acid concentrations, M_{T_1} and M_{T_2}, indicates the same physical state of the nucleic acid; i.e., the degree of binding, $\sum\Theta_i$, and the free rat pol β concentration, P_F, must be the same. The values of $\sum\Theta_i$ and P_F are then related to the total protein concentrations, P_{T_1} and P_{T_2}, and the total nucleic acid concentrations, M_{T_1} and

M_{T_2}, at the same value of ΔF_{obs} by

$$\sum\Theta_i = \frac{(P_{T_2} - P_{T_1})}{(M_{T_2} - M_{T_1})} \quad (8)$$

and

$$P_F = P_{T_X} - (\sum\Theta_i)M_{T_X} \quad (9)$$

where $x = 1$ or 2 (*33*−*37*).

Analysis of Rat Pol β−*Unmodified dsDNA Complexes Using the MCT Method*. Determination of binding parameters for the rat pol β−unmodified dsDNA oligomer complex has been performed using the MCT method with the dsDNA oligomer labeled with CP as a reference fluorescent nucleic acid (*16*, *35*). Briefly, if the fluorescent reference nucleic acid at total concentration, M_{T_R}, is titrated with the protein in the absence of a competing nonfluorescent nucleic acid of total concentration, M_S, the total concentration of the protein, P_{T_1}, at which a given fluorescence change, ΔF_i, is observed is described by the mass conservation relationship

$$P_{T_1} = (\sum\Theta_i)_R M_{T_R} + P_F \quad (10)$$

where $(\sum\Theta_i)_R$ and P_F are the degree of binding of the protein on the reference fluorescent nucleic acid and the free protein concentration, respectively. The total concentration of the protein, P_{T_2}, at which the same ΔF_i is observed at the same M_{T_R} in the presence of the competing nonfluorescent nucleic acid is described by

$$P_{T_2} = (\sum\Theta_i)_S M_S + (\sum\Theta_i)_R M_{T_R} + P_F \quad (11)$$

where $(\sum\Theta_i)_S$ is the degree of binding of the protein on the nonfluorescent competing oligomer. Subtracting eq 10 from eq 11 and rearranging provides eq 12, which allows us to determine the degree of binding of the protein on the competing, nonfluorescent ssDNA oligomer (*35*)

$$(\sum\Theta_i)_S = \frac{P_{T_2} - P_{T_1}}{M_S} \quad (12)$$

RESULTS

Site-Size of the Rat Pol β−*dsDNA Complex*. Binding of rat pol β to the dsDNA is not accompanied by large enough changes of the protein fluorescence that would allow us to examine complex binding process. However, we have found that association of the enzyme with a dsDNA oligomer labeled at the 5′ end of one of the ssDNA strands with the coumarin derivative, CP (Figure 1a, substrate A), is accompanied by a strong (∼150%) increase of the nucleic acid fluorescence. Such a large emission change provides an excellent signal to monitor the polymerase−dsDNA interactions and to perform high-resolution measurements of the enzyme−dsDNA complex formation. To address the energetics of the polymerase interactions with the dsDNA, we selected the dsDNA 10-mer, containing random sequences of bases. The oligomer is twice as large as the site-size of five nucleotide residues of the enzyme−ssDNA complex in the (pol β)$_5$ binding mode (*12*−*15*). Moreover, the selected dsDNA oligomer allows us to perform titrations over large DNA and protein concentration ranges, avoiding the precipitation of the sample.

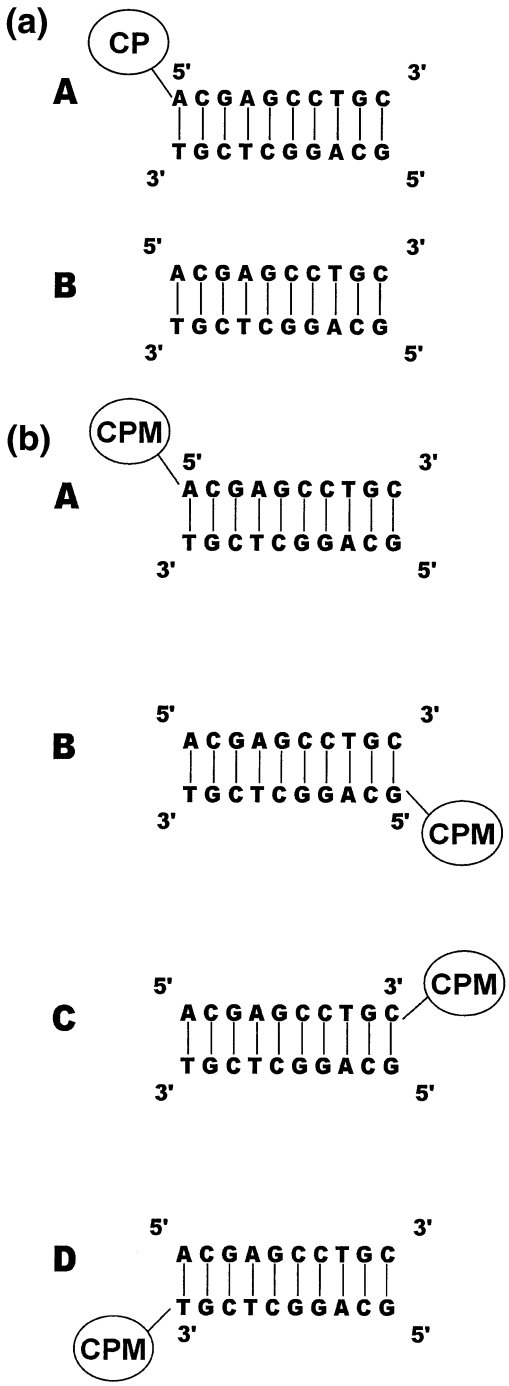

FIGURE 1: (a) Primary structure of the dsDNA 10-mer that is used to examine the interactions of rat pol β with the dsDNA. The modified DNA substrate (A) differs from the unmodified DNA oligomer (B) by having a coumarin derivative, CP, attached to the 5′ end of one of the ssDNA strands that provide the signal to monitor the polymerase binding. (b) dsDNA oligomers used in the fluorescence energy transfer studies of the rat pol β−dsDNA complex topology. In oligomers A and B, the nucleic acids have a coumarin derivative, CPM, attached to the 5′ end of one of the ssDNA strands. In oligomers C and D, the CPM marker is attached to the 3′ end of one of the ssDNA strands.

Fluorescence titrations of the CP-labeled dsDNA 10-mer with rat pol β, at two different nucleic acid concentrations, in buffer C (pH 7.0, 10 °C), containing 100 mM NaCl, are shown in Figure 2a. At higher nucleic acid concentration, a

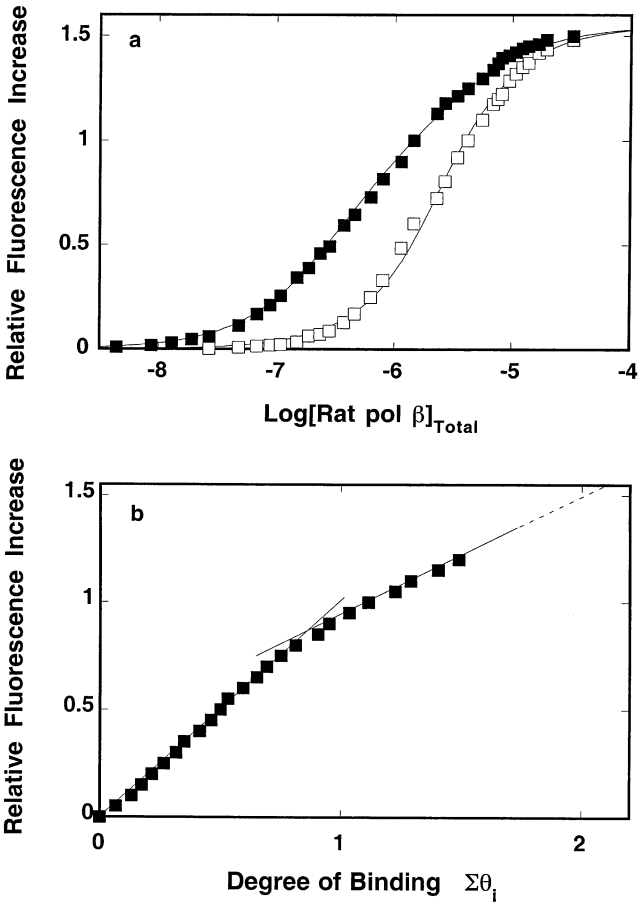

FIGURE 2: (a) Fluorescence titrations of the dsDNA 10-mer (Figure 1a, substrate A) with the rat pol β ($\lambda_{ex} = 435$ nm; $\lambda_{em} = 480$ nm) in buffer C (pH 7.0, 10 °C), containing 100 mM NaCl, at two different nucleic acid concentrations: (■) 1.11×10^{-7} M; (□) 2.22×10^{-6} M (oligomer). The solid lines are computer fits of the titration curves using eqs 13−15 for the cooperative binding of two enzyme molecules to the nucleic acid lattice with the site-size of the complex $n = 5$ base pairs, the intrinsic binding constant $K = 7.8 \times 10^5$ M^{-1}, cooperative interaction parameter $\omega = 2.3$, relative fluorescence change $\Delta F_1 = 0.95$, and $\Delta F_2 = 0.6$ (see text for details). (b) Dependence of the relative fluorescence of the dsDNA oligomer, ΔF, upon the average number of bound pol β molecules (■). The solid line follows the experimental points and has no theoretical basis. The dashed line is the extrapolation of ΔF to the maximum value of $\Delta F_{max} = 1.55$.

given relative fluorescence increase, ΔF, is reached at higher polymerase concentrations. This results from the fact that at higher DNA concentration, more protein is required to obtain the same degree of binding, $\sum\Theta_i$. The selected DNA concentrations provide separation of binding isotherms up to $\Delta F \approx 1.35$. To obtain thermodynamically rigorous binding parameters independently of any assumption about the relationship between the observed signal and the degree of binding, $\sum\Theta_i$, titration curves in Figure 2a have been analyzed using the approach outlined in Materials and Methods (*33*−*37*).

Figure 2b shows the dependence of the observed relative fluorescence increase, ΔF, as a function of the average degree of binding, $\sum\Theta_i$, of rat pol β. The plot is nonlinear and shows two binding phases. In the first phase, a single molecule of the polymerase binds with the relative fluorescence increase, ΔF, reaching a value of ~0.85 at $\sum\Theta_i \approx 0.9$. Extrapolation of the second phase to the maximum value of the fluorescence increase, $\Delta F_{max} = 1.55 \pm 0.1$, gives the maximum value of $\sum\Theta_i = 2.2 \pm 0.1$. Thus, at saturation, two rat pol β molecules bind to the dsDNA 10-mer. Experiments at different salt concentrations provide the same dependence of the observed signal as a function of the average degree of binding, indicating that $\sum\Theta_i$ and the observed fluorescence changes are independent of the salt concentration (see below).

The data in Figure 2 reveal two fundamental aspects of the pol β−dsDNA interactions. First, at saturation, two pol β molecules bind to the 10-mer. Analogous binding studies have been performed with longer dsDNA oligomers (data not shown). Two enzyme molecules bind to 12- and 14-mer, while an addition of an extra single base pair causes three polymerase molecules to bind to the 15-mer. Moreover, at higher salt concentrations and/or in the presence of magnesium, the two binding phases merge into one cooperative binding process (see below). This is very different from the behavior of the pol β in its complexes with the ssDNA where two binding phases existed at any examined solution conditions (*12*−*15*). Therefore, the observed behavior strongly indicates that the enzyme forms a single type of complex with the dsDNA and requires only 5 ± 1 base pairs to form a stable complex with the nucleic acid (*12*−*15*). In other words, the obtained data indicate that the site-size of the pol β−dsDNA complex is $n = 5 \pm 1$ base pairs (Figure 2b). Experiments with oligomers longer than ~15 base pairs were hindered by the fact that their complexes with pol β precipitate, particularly at higher enzyme and/or DNA concentrations (data not shown). However, the obtained intrinsic binding constants and cooperative interaction parameters with the examined longer dsDNA oligomers are, within experimental accuracy, the same as those determined for the dsDNA 10-mer, indicating that there is not a detectable "end effect" on the enzyme binding to the DNA. This is in excellent agreement with our previous studies of interactions between rat and human pol β with various ss and gapped DNA oligomers where no end effect in the enzyme binding was observed (*12*−*15*).

Second, the stoichiometry of the rat pol β binding to the dsDNA 10-mer is not affected by a ~20-fold increase of the dsDNA oligomer concentration (Figure 2a). Such independence of the rat pol β−dsDNA stoichiometry upon DNA oligomer concentrations provides strong thermodynamic evidence that only one of the two DNA-binding subsites of the enzyme engages in interactions with the dsDNA (*12*−*15*, *36*). If the second DNA-binding subsite binds the dsDNA oligomer, its affinity must be at least ~100-fold lower than the observed affinity. The ~20-fold increase of the 10-mer concentration would detect such weak interactions with the second DNA binding subsite by showing a dramatic decrease in the stoichiometry of the complex. This is not experimentally observed. Therefore, the obtained data indicate that the enzyme binds the dsDNA using only one of its DNA binding-subsites in any of the formed complexes (see below).

Statistical Thermodynamic Model of Rat Pol β Binding to the dsDNA 10-mer. The simplest statistical thermodynamic model that describes the rat pol β binding to the dsDNA 10-mer is defined by the partition function, Z_N, as (*12*, *16*, *38*, *39*)

$$Z_N = 1 + (N - n + 1)KP_F + \omega(KP_F)^2 \qquad (13)$$

Table 1: Intrinsic Binding Constants, K, Cooperativity Parameters, ω, and Spectroscopic Parameters for the Binding of Rat Pol β to the dsDNA 10-mer (Figure 1a, Substrate A) in Buffer C (pH 7.0, 10 °C) Containing Different NaCl or NaBr Concentrations[a]

NaCl (mM)	K (M^{-1})	ω	ΔF_1	ΔF_2
100	$(7.8 \pm 0.8) \times 10^5$	2.3 ± 0.5	0.95 ± 0.05	0.6 ± 0.05
151	$(1.5 \pm 0.2) \times 10^5$	9 ± 2	0.95 ± 0.05	0.6 ± 0.05
201	$(5 \pm 0.6) \times 10^4$	17 ± 4	0.95 ± 0.05	0.6 ± 0.05
252	$(1.8 \pm 0.3) \times 10^4$	30 ± 7	0.95 ± 0.05	0.6 ± 0.05
NaBr (mM)	K (M^{-1})	ω	ΔF_1	ΔF_2
50	$(1.2 \pm 0.2) \times 10^7$	0.28 ± 0.08	0.87 ± 0.05	0.3 ± 0.05
75	$(8 \pm 1) \times 10^5$	4.5 ± 1.2	0.87 ± 0.05	0.3 ± 0.05
102	$(1.9 \pm 0.8) \times 10^5$	14 ± 3	0.87 ± 0.05	0.3 ± 0.05
150	$(3.5 \pm 0.8) \times 10^4$	40 ± 8	0.87 ± 0.05	0.3 ± 0.05

[a] Errors are standard deviations determined using three to four independent titration experiments.

where N is the total number of base pairs in the oligomer ($N = 10$), n is the site-size of the pol β−dsDNA complex, ω is the parameter characterizing the cooperative interactions between the bound protein molecules, and P_F is the free pol β concentrations (*39*−*41*). The degree of binding, $\sum\Theta_i$, is then described by

$$\sum\Theta_i = \frac{[(N - n + 1)KP_F + 2\omega(KP_F)^2]}{K_N} \qquad (14)$$

The observed relative fluorescence increase, ΔF, of the nucleic acid is then

$$\Delta F = \Delta F_1\left[\frac{(N - n + 1)KP_F}{Z_N}\right] + (\Delta F_1 + \Delta F_2)\left[\frac{\omega(KP_F)^2}{Z_N}\right] \qquad (15)$$

where ΔF_1 and ΔF_2 are relative molar fluorescence increases accompanying the binding of the first and second rat pol β molecule to the dsDNA 10-mer.

The determination of all interaction and spectroscopic parameters of this binding system can be achieved by applying the following strategy. The value of ΔF_1 can be obtained as the slope, $\Delta F_1 = \partial\Delta F/\partial(\sum\Theta_i)$, of the initial part of the plot in Figure 2b, which provides $\Delta F_1 = 0.95 \pm 0.05$ (*12*−*15*). The determination of ΔF_2 is based on the fact that the final complex, at saturation, must contain two rat pol β molecules bound to the dsDNA, i.e., $\Delta F_{max} = \Delta F_1 + \Delta F_2$. Therefore, the determined value of $\Delta F_{max} = 1.55 \pm 0.1$ provides $\Delta F_2 = 0.6 \pm 0.05$. Thus, there are only two remaining parameters that must be determined: K and ω. The solid lines in Figure 2a are the computer fits of the experimental isotherm to eq 15 with the intrinsic binding constant, K, and cooperativity parameter, ω, as the fitting parameters. The obtained values of the binding and spectroscopic parameters are included in Table 1. It is clear that the model (eqs 13−15) provides an excellent description of the experimentally observed binding process.

Binding of Rat Pol β to Unmodified dsDNA Oligomer. Macromolecular Competition Titrations. Using the MCT method outlined in the Materials and Methods, we can quantitatively address the rat pol β binding to unmodified dsDNA (Figure 1a, substrate B) (*35*). In these studies, we use the dsDNA labeled with CP (Figure 1a, substrate A) as a reference fluorescent nucleic acid. Fluorescence titration

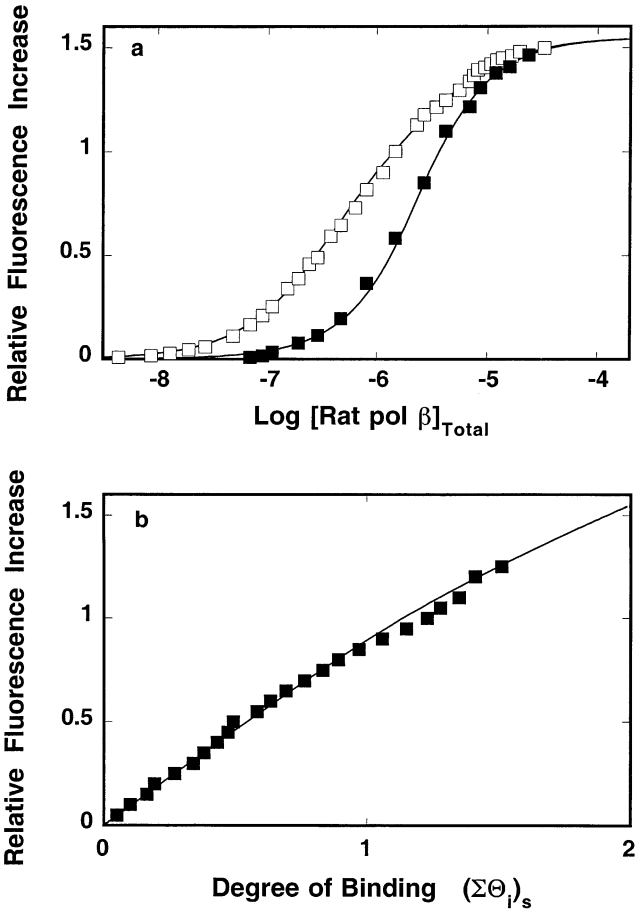

FIGURE 3: (a) Fluorescence titrations of dsDNA 10-mer ($\lambda_{ex} = 435$ nm; $\lambda_{em} = 480$ nm) with the rat pol β in buffer C (pH 7.0, 10 °C), containing 100 mM NaCl, in the presence of unmodified dsDNA 10-mer (□). For comparison, the fluorescence titration of only the fluorescent oligomer, in the same solution conditions, is included (■). The solid lines are computer fits of the experimental fluorescence binding isotherms using the macromolecule competition titration method (MCT) as outlined in Materials and Methods (*35*). The concentration of fluorescent dsDNA oligomer and unmodified nucleic acid are 1.11×10^{-7} and 2.22×10^{-6} M (oligomer), respectively. (b) Dependence of the observed fluorescence increase, ΔF, of the labeled dsDNA oligomer upon the degree of binding, $(\sum\Theta_i)_S$, of the rat pol β−unmodified dsDNA oligomer complex (■). The quantitative determination of $(\sum\Theta_i)_S$ has been performed using the MCT method described in Materials and Methods (*35*). The solid line is the computer simulation of the dependence of ΔF upon $(\sum\Theta_i)_S$, using the determined binding parameters for both nucleic acid lattices (Table 1).

of the CP-labeled dsDNA 10-mer (1.11×10^{-7} M (oligomer)) with rat pol β in the presence of unlabeled dsDNA 10-mer (2.22×10^{-6} M (oligomer)) in buffer C (pH 7.0, 10 °C), containing 100 mM NaCl, is shown in Figure 3a. For comparison, we also include the titration curve of the labeled oligomer alone with the enzyme at the same fluorescent nucleic acid concentration as in the titration performed in the presence of unmodified nucleic acid. In the presence of the competing, nonfluorescent oligomer, the binding isotherm is shifted toward higher protein concentrations because of the simultaneous binding of the protein to the fluorescent and the unmodified oligomer. On the other hand, at the same value of the fluorescence increase of the labeled DNA, independent of the presence of the competing unmodified oligomer, the physical state of the fluorescent nucleic acid

must be the same; i.e., the values of $\sum\Theta_i$ and the free protein concentration, [rat pol β]$_F$, must be the same (*35*). The degree of binding of the protein on the unmodified ssDNA, $(\sum\Theta_i)_S$, is also the sole, unique function of the [rat pol β]$_F$. Therefore, at a given value of ΔF, the value of $(\sum\Theta_i)_S$ must be the same, independent of the concentration of the unmodified nucleic acid. The degree of binding, $(\sum\Theta_i)_S$, can then be obtained using eq 12 (*35*).

The dependence of the fluorescence increase of the reference fluorescent dsDNA oligomer as a function of the average binding density, $(\sum\Theta_i)_S$, of the rat pol β−unmodified complex is shown in Figure 3b. The plot is close to being linear, an indication that the enzyme binds unmodified DNA with very similar affinity as modified oligomer (*35*). Extrapolation to the maximum observed fluorescence change, $\Delta F_{max} = 1.55 \pm 0.05$, gives $(\sum\Theta_i)_S = 2 \pm 0.2$, which indicates that two pol β molecules bind to the unmodified dsDNA 10-mer, i.e., with the same stoichiometry as obtained for the CP-labeled DNA (Figure 2b). The solid line in Figure 3a is the computer fit of the experimental titration curve for the simultaneous binding of rat pol β to two competing nucleic acids, each binding system described by the partition function defined by eq 13 (*35*). Because binding parameters for the CP-labeled DNA have been independently determined (Table 1), there are only two parameters (the intrinsic binding constant, K_S, and the cooperativity parameter, ω_S, for the unlabeled DNA) that remain to be determined. The solid line in Figure 3a is a computer fit of the experimental curve using $K_S = (7.7 \pm 1) \times 10^5$ M^{-1} and $\omega_S = 2.3 \pm 0.5$. Thus, the binding of the enzyme to unmodified dsDNA is characterized, within experimental accuracy, by the same parameters as the binding to the modified DNA in corresponding solution conditions (Table 1). In other words, the presence of the CP moiety does not affect to any detectable extent the enzyme interactions with the examined CP-labeled dsDNA 10-mer.

Salt Effect on the Intrinsic Affinity and Cooperativity in Rat Pol β−dsDNA Interactions. Fluorescence titrations of the CP-labeled dsDNA 10-mer with rat pol β, in buffer C (pH 7.0, 10 °C) containing different NaCl concentrations, are shown in Figure 4a. Analogous titrations in the presence of NaBr are shown in Figure 4b. The maximum fluorescence increase at saturation, ΔF_{max}, is not affected by the increasing [NaCl], indicating that the salt does not affect the structure of the enzyme−nucleic acid complex. Note that a very different behavior was observed for pol β interactions with the ssDNA, where the fluorescence of etheno derivatives of the DNA strongly decreases with the increasing [NaCl] (*12*). The solid lines in parts a and b of Figure 4 are computer fits of the experimental isotherms to eq 15, with two fitting parameters (intrinsic binding constant, *K*, and the cooperativity parameter, ω). The obtained parameters are included in Table 1.

There is a striking difference between the behavior of intrinsic affinities and cooperative interactions in response to the changing salt concentration in solution. The intrinsic affinities strongly decrease with the increasing concentration of both NaCl and NaBr, indicating that net ion release accompanies the intrinsic interactions with the nucleic acid (*42*−*44*). On the other hand, the cooperativity parameter, ω, strongly increases with the salt concentration, indicating that net ion uptake, not a release, accompanies the cooperative interactions (Table 1). Parts c and d of Figure 4 show the dependence of the logarithm of rat pol β intrinsic binding constant, *K*, upon the logarithm of the NaCl and NaBr concentrations (log−log plots) (*42*−*44*). The plots are linear and characterized by the slopes $\partial \log K/\partial \log [NaCl] = -4 \pm 0.5$ and $\partial \log K/\partial \log [NaBr] = -5.3 \pm 0.5$, respectively. Thus, a net release of about four to five ions accompanies the intrinsic interaction between the enzyme and the dsDNA. However, a higher slope is observed in the presence of NaBr, i.e., where chloride anions are replaced by bromide. Such a difference indicates that both cations and anions participate in the ion exchange resulting from the pol β binding to the dsDNA (*42*−*44*) (see Discussion).

The dependence of the logarithm of the cooperativity parameter, ω, upon the logarithm of the NaCl and NaBr concentrations is also included in parts c and d of Figure 4. The plots are linear; however, contrary to the intrinsic binding constants, the plots are characterized by positive slopes, $\partial \log \omega/\partial \log [NaCl] = 2.8 \pm 0.4$ and $\partial \log \omega/\partial \log [NaBr] = 4.5 \pm 0.5$, respectively. Thus, the cooperative interactions are accompanied by a net multiple-ion uptake. Moreover, there is a significant difference between the slopes obtained in the presence of NaCl and NaBr, with the slope $\partial \log \omega/\partial \log [NaBr]$ being a factor of ∼1.6 higher than $\partial \log \omega/\partial \log[NaCl]$. The large difference between the slopes of log−log plots, observed in the presence of NaCl and NaBr, indicates that both cations and anions significantly contribute to the net ion uptake accompanying the cooperative interactions (*42*−*44*) (see Discussion).

Salt Effect on Rat Pol β−dsDNA Interactions in the Presence of Magnesium. As we pointed out, magnesium has a profound effect on interactions of pol β and its 8-kDa domain with the ssDNA and on stoichiometries of formed complexes (*12*, *16*). In the case of the dsDNA, the presence of magnesium does not affect the stoichiometries of complexes. However, the Mg^{2+} effect is reflected in different salt effects on the enzyme interactions with the nucleic acid. Fluorescence titrations of the CP-labeled dsDNA oligomer with rat pol β, in buffer C (pH 7.0, 10 °C) containing different NaCl concentrations and 1 mM $MgCl_2$, are shown in Figure 5a. Analogous titrations, performed in the presence of NaBr, are shown in Figure 5b. The solid lines are computer fits of the experimental titration curves using eq 15. The obtained binding parameters are included in Table 2.

The dependence of the logarithm of the intrinsic binding constant upon the logarithm of [NaCl] and [NaBr] is shown in parts c and d of Figure 5. Within experimental accuracy, the plots are linear and characterized by the slopes $\partial \log K/\partial \log [NaCl] = -5.1 \pm 0.5$ and $\partial \log K/\partial \log [NaBr] = -4.8 \pm 0.5$, respectively. The values of the slopes indicate that in the presence of NaCl magnesium moderately increases the net number of ions released accompanying intrinsic binding to the dsDNA. On the other hand, the slope $\partial \log K/\partial \log [NaBr]$, although within the experimental error, is slightly decreased in the presence of Mg^{2+}. These are unexpected results if the protein, magnesium, and sodium ions simply compete for the binding sites on the nucleic acid (*42*−*44*). Moreover, the different effect on the net number of released ions, depending on the type of anion in solution, indicates that Mg^{2+} also affects the anion exchange accompanying the intrinsic interactions between the protein and

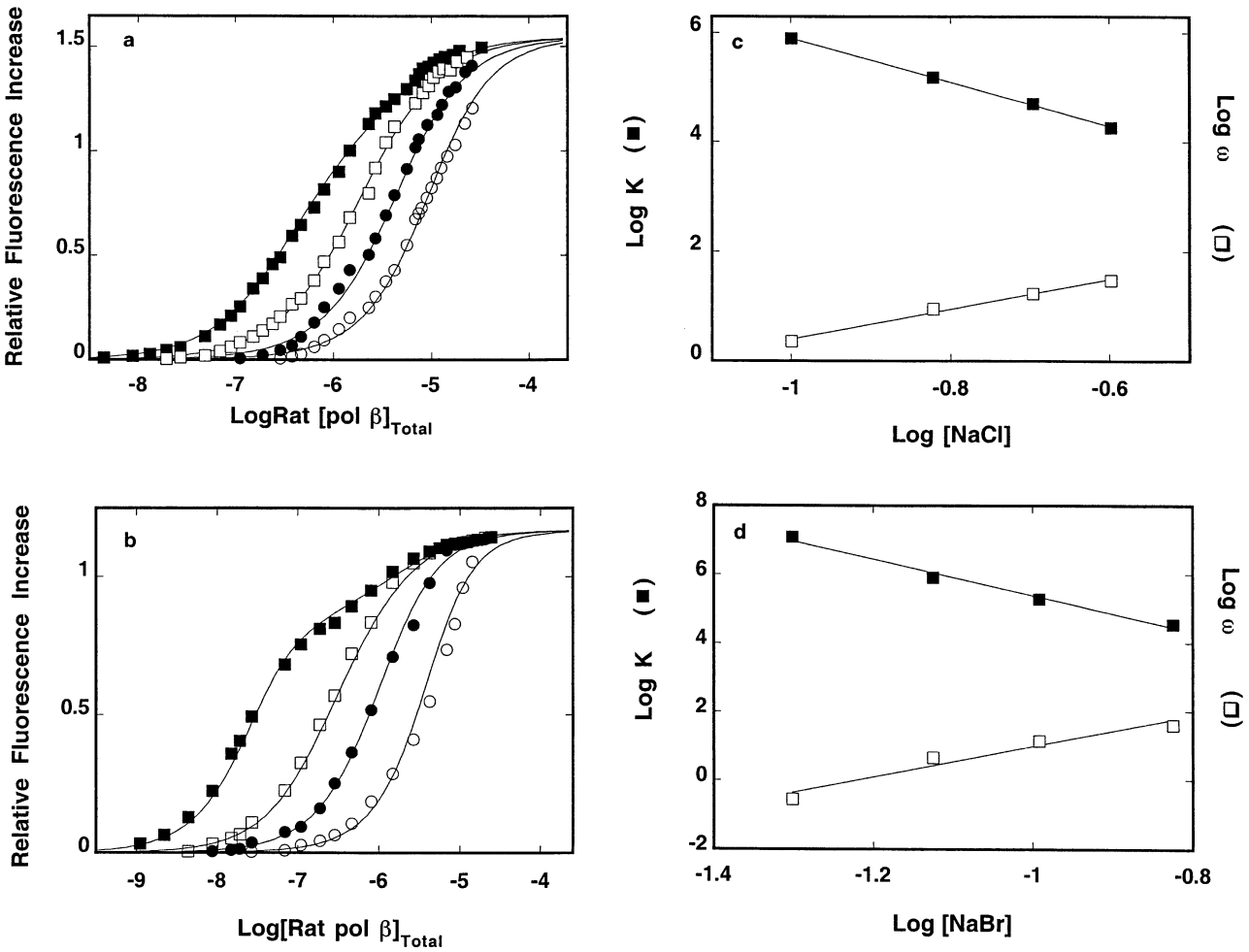

FIGURE 4: (a) Fluorescence titrations of the dsDNA oligomer with rat pol β (λ_{ex} = 435 nm; λ_{em} = 480 nm) in buffer C (pH 7.0, 10 °C) containing different NaCl concentrations: 100 mM (■), 151 mM (□), 201 mM (●), 252 mM (○). The solid lines are computer fits of the titration curves using eqs 13−15 for the cooperative binding of two enzyme molecules to the nucleic acid lattice with the site-size of the complex n = 5 base pairs. The obtained binding and spectroscopic parameters are included in Table 1. (b) Fluorescence titrations of the dsDNA oligomer with rat pol β (λ_{ex} = 435 nm; λ_{em} = 480 nm) in buffer C (pH 7.0, 10 °C) containing different NaBr concentrations: 50 mM (■), 75 mM (□), 102 mM (●), 150 mM (○). The solid lines are computer fits of the titration curves using eqs 13−15 for the cooperative binding of two enzyme molecules to the nucleic acid lattice with the site-size of the complex n = 5 base pairs. The obtained binding and spectroscopic parameters are included in Table 1. (c) Dependence of the logarithm of the intrinsic binding constants, K (■), and cooperative interaction parameter, ω (□), upon the logarithm of NaCl concentration, determined from titrations shown in panel a. The solid lines are linear least-squares fits that provide the slopes $\partial \log K/\partial \log [NaCl] = -4.04$ and $\partial \log \omega/\partial \log [NaCl] = 2.8$. (d) Dependence of the logarithm of the intrinsic binding constants, K (■), and cooperative interaction parameter, ω (□), upon the logarithm of NaBr concentration, determined from titrations shown in panel b. The solid lines are linear least-squares fits that provide the slopes $\partial \log K/\partial \log [NaBr] = -5.3$ and $\partial \log \omega/\partial \log [NaBr] = 4.5$. The concentration of the nucleic acid in all experiments is 1.11×10^{-7} M (oligomer).

the dsDNA. This is similar to the analogous behavior of the isolated 8-kDa domain of rat pol β in its interactions with the ssDNA, where the presence of Mg^{2+} affects the ion exchange processes accompanying intrinsic interactions (*12*, *16*) (see Discussion).

A significant effect of Mg^{2+} is also observed for the cooperative interactions between bound pol β molecules. The dependence of the logarithm of the cooperative interactions parameter, ω, upon the logarithm of [NaCl] and [NaBr] is included in parts c and d of Figure 5. The values of ω significantly increase with increasing salt concentration (Tables 1 and 2). The obtained values of the positive slopes, $\partial \log \omega/\partial \log [NaCl]$ and $\partial \log \omega/\partial \log [NaBr]$, are 4.5 ± 0.5 and 3.5 ± 0.4, respectively. Thus, multiple-ion uptake accompanies the cooperative interactions. As a result, the binding process becomes strongly cooperative at high salt concentrations. However, contrary to the data obtained in the absence of magnesium (parts c and d of Figure 4, Table 1), significantly larger ion uptake occurs in the presence of chloride anions rather than bromide anions (see Discussion).

Topology of the Rat Pol β−dsDNA Complex. To obtain further insight about the topology of the rat pol β−dsDNA complex, we performed fluorescence energy transfer measurements of the formed complex. We utilize the fact that rat pol β has a single tryptophan residue, W325, located on the surface of the 31-kDa domain (*7*). This residue can serve as a single fluorescence energy transfer donor to a single acceptor located on the dsDNA oligomer. Thus, measurement of the fluorescence energy transfer efficiency will provide unique information about the location of the bound dsDNA oligomer with respect to the 8- and 31-kDa domain of the enzyme. The series of DNA substrates selected for these studies is depicted in Figure 1b. They have the same primary structure as the oligomer used in the thermodynamic studies

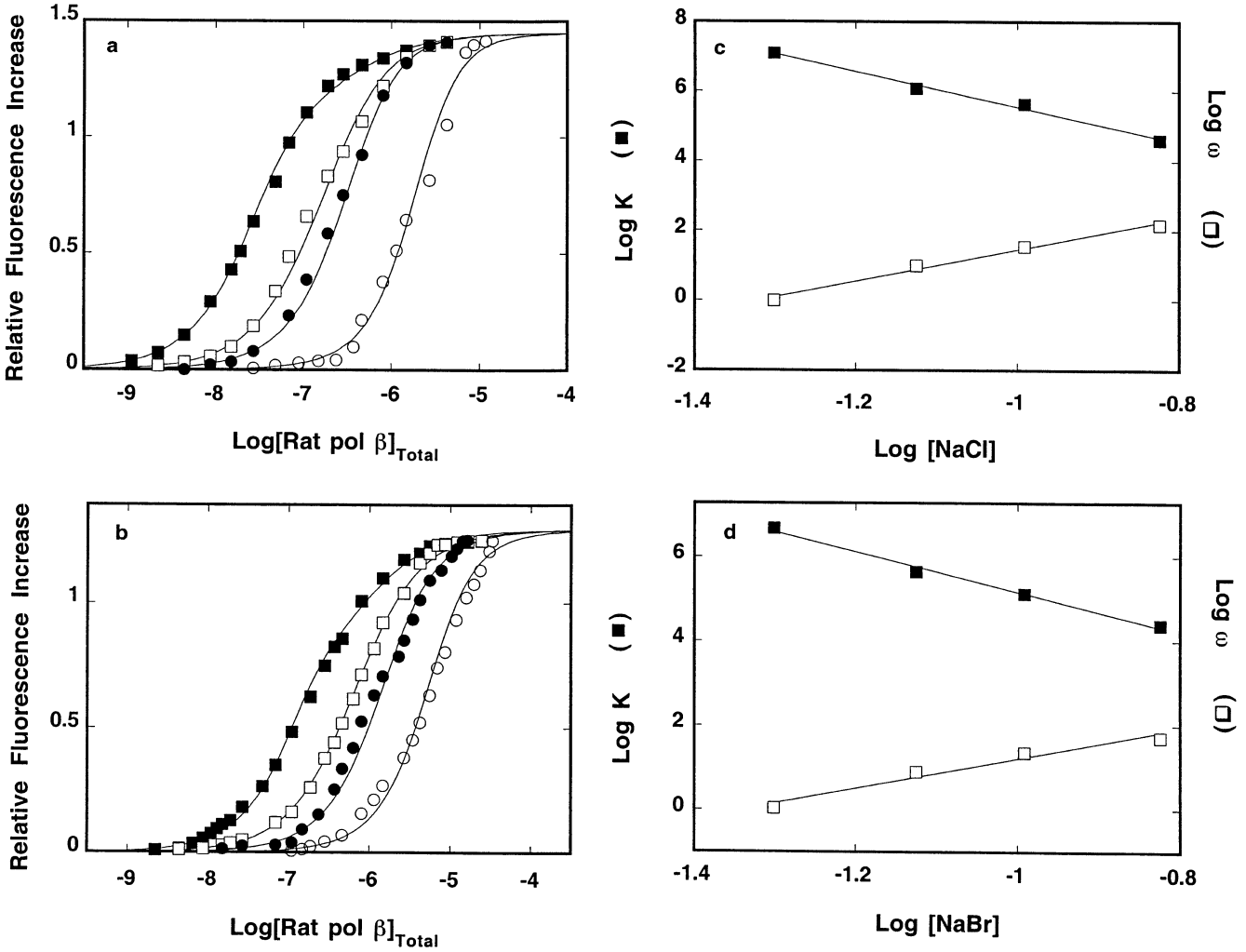

FIGURE 5: (a) Fluorescence titrations of the dsDNA oligomer with rat pol β (λ_{ex} = 435 nm; λ_{em} = 480 nm) in buffer C (pH 7.0, 10 °C) containing 1 mM $MgCl_2$ and different NaCl concentrations: 50 mM (■), 75 mM (□), 102 mM (●), 150 mM (○). The solid lines are computer fits of the titration curves using eqs 13−15 for the cooperative binding of two enzyme molecules to the nucleic acid lattice with the site-size of the complex $n = 5$ base pairs. The obtained binding and spectroscopic parameters are included in Table 2. (b) Fluorescence titrations of the dsDNA oligomer with rat pol β (λ_{ex} = 435 nm; λ_{em} = 480 nm) in buffer C (pH 7.0, 10 °C) containing 1 mM $MgCl_2$ and different NaBr concentrations: 50 mM (■), 75 mM (□), 102 mM (●), 150 mM (○). The solid lines are computer fits of the titration curves using eqs 13−15 for the cooperative binding of two enzyme molecules to the nucleic acid lattice with the site-size of the complex $n = 5$ base pairs. The obtained binding and spectroscopic parameters are included in Table 2. (c) Dependence of the logarithm of the intrinsic binding constants, K (■), and cooperative interaction parameter, ω (□), upon the logarithm of NaCl. The solid lines are linear least-squares fits that provide the slopes $\partial \log K/\partial \log [NaCl] = -5.1$ and $\partial \log \omega/\partial \log [NaCl] = 4.5$. (d) Dependence of the logarithm of the intrinsic binding constants, K (■), and cooperative interaction parameter, ω (□), upon the logarithm of NaBr. The solid lines are linear least-squares fits that provide the slopes $\partial \log K/\partial \log [NaBr] = -4.8$ and $\partial \log \omega/\partial \log [NaBr] = 3.5$. The concentration of the nucleic acid in all experiments is 1.11×10^{-7} M (oligomer).

described above. Each DNA substrate has a fluorescent marker, 7-methoxycoumarin (CPM), attached through a six-carbon linker at the 5′ or 3′ terminus of one of the ssDNA strands. Thus, there are four possible locations of the CPM residue on the dsDNA oligomer (Figure 1b). The binding parameters of the enzyme to the CPM-labeled dsDNA are indistinguishable from the binding parameters obtained for the CP-labeled DNA substrates or unmodified DNA (data not shown), in excellent agreement with the finding that the coumarin label does not affect to any detectable extent the energetics of enzyme interactions with the examined dsDNA oligomers (parts a and b of Figure 3).

Unlike the CP coumarin derivative used in the binding studies (see above), CPM has absorption maximum at ~355 nm strongly overlapping with the fluorescence emission spectrum of the polymerase. The overlap of an absorption spectrum of an acceptor with the emission spectrum of a donor is a condition for the fluorescence resonance energy transfer to occur (*22*, *23*, *27*). The fluorescence emission spectrum of rat pol β (λ_{ex} = 295 nm) and the emission spectrum of CPM-labeled dsDNA oligomer (Figure 1b, substrate A) in buffer C (pH 7.0, 10 °C), containing 40 mM NaCl, are shown in Figure 6a. There is a large overlap of the donor emission (pol β) with the acceptor absorption spectrum, indicating that efficient fluorescence energy transfer can occur if the tryptophan and CPM are in proximity. The overlap integral is $J = 2.39 \times 10^{-13}$ M^{-1} cm^3. Using the determined quantum yield of the rat pol β tryptophan $\phi_d = 0.044$ and eq 6, we determined that the Förster critical distance, R_0, for the CPM on the dsDNA and the rat pol β tryptophan is 21.6 Å.

Table 2: Intrinsic Binding Constants, K, Cooperativity Parameters, ω, and Spectroscopic Parameters for the Binding of Rat Pol β to the DsDNA 10-mer (Figure 1a, Substrate A) in Buffer C (pH 7.0, 10 °C) Containing 1 mM $MgCl_2$ and Different NaCl or NaBr Concentrations[a]

NaCl (mM)	K (M^{-1})	ω	ΔF_1	ΔF_2
50	$(1.2 \pm 0.2) \times 10^7$	1 ± 0.2	1.2 ± 0.05	0.25 ± 0.05
75	$(1.2 \pm 0.2) \times 10^6$	10 ± 2	1.2 ± 0.05	0.25 ± 0.05
102	$(4.4 \pm 0.4) \times 10^5$	35 ± 7	1.2 ± 0.05	0.25 ± 0.05
150	$(4.0 \pm 0.4) \times 10^4$	150 ± 30	1.2 ± 0.05	0.25 ± 0.05
NaBr (mM)	K (M^{-1})	ω	ΔF_1	ΔF_2
50	$(5 \pm 0.7) \times 10^6$	1.1 ± 0.3	0.85 ± 0.05	0.45 ± 0.05
75	$(4.4 \pm 0.5) \times 10^5$	8 ± 2	0.85 ± 0.05	0.45 ± 0.05
102	$(1.3 \pm 0.2) \times 10^5$	23 ± 5	0.85 ± 0.05	0.45 ± 0.05
150	$(2.4 \pm 0.7) \times 10^4$	53 ± 10	0.85 ± 0.05	0.45 ± 0.05

[a] Errors are standard deviations determined using three to four independent titration experiments.

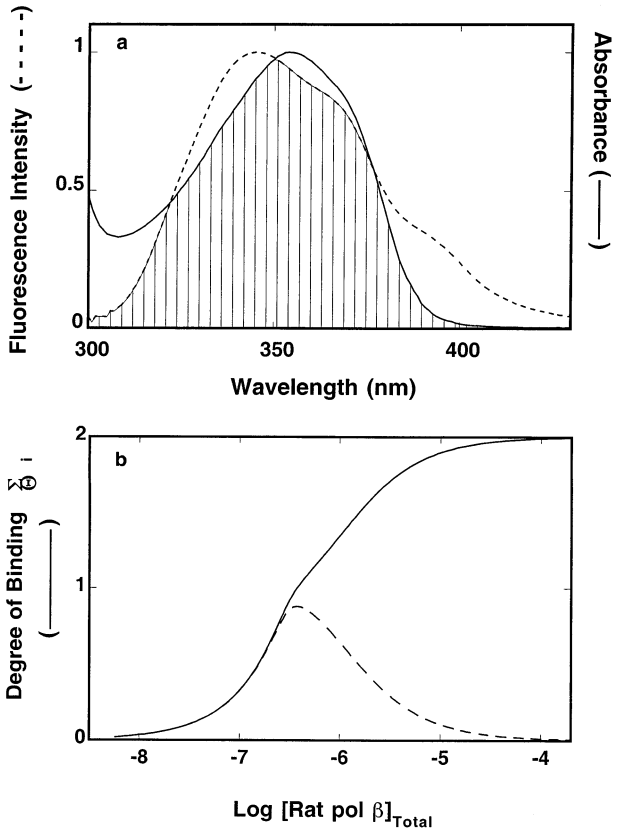

FIGURE 6: (a) Spectral overlap between single tryptophan emission of rat pol β (donor) and absorption spectrum of CPM moiety at the 5′ end of the dsDNA 10-mer (acceptor) in buffer C (pH 7.0, 10 °C) containing 40 mM NaCl: rat pol β emission spectrum (- - -) ($\lambda_{ex} = 295$ nm), absorption spectrum of 5′-CPM-dsDNA 10-mer (Figure 1b, substrate A) (−). (b) Computer simulation of the dependence of the average total degree of binding, $\sum\Theta_i$ (−) and the fraction of the pol β−dsDNA complex (- - -), with a single molecule of the enzyme bound to the nucleic acid, on the total concentration of the enzyme. The concentration of the DNA oligomer is 3×10^{-7} M (oligomer). The simulation was performed using intrinsic binding constant $K = 3.2 \times 10^7$ M^{-1} and cooperativity parameter $\omega = 0.18$.

Because we want to determine the location of the dsDNA oligomer with respect to the 8- and 31-kDa domain in the complex with a single pol β molecule, measurements have to be performed in conditions where the complex with one polymerase molecule bound to the dsDNA oligomer dominates the population distribution. This can be achieved by using thermodynamic parameters characterizing complex formation and appropriate concentrations of the enzyme and nucleic acid and by utilizing the fact that cooperative interactions are strongly salt-dependent (Table 1, Figure 4c). In buffer C (pH 7.0, 10 °C), containing 40 mM NaCl, the intrinsic binding constant K is $3.2 \pm 0.3 \times 10^7$ M^{-1} and ω is 0.18 ± 0.03; i.e., the binding is characterized by a significant negative cooperativity allowing the required separation of the 1:1 complex from the 1:2 complex. The computer simulation of the dependence of the total average degree of binding, $\sum\Theta_i$, and the fraction of the 1:1 complex as a function of the [rat pol β]$_T$, using eqs 13−15, are shown in Figure 6b. The selected total concentration of the nucleic acid is 3×10^{-7} M. It is clear that at the selected solution conditions and [DNA]$_T$, the 1:1 complex constitutes ∼90−95% of the total complex population at [rat pol β]$_T = 5 \times 10^{-7}$ M.

Fluorescence emission spectra of rat pol β (5×10^{-7} M) ($\lambda_{ex} = 295$ nm) in the absence and presence of CPM-labeled dsDNA oligomer (3×10^{-7} M) (Figure 1b, substrate A) and the emission spectrum of the CPM-labeled DNA in the absence of the protein ($\lambda_{ex} = 295$ nm) in buffer C (pH 7.0, 10 °C), containing 40 mM NaCl, are shown in Figure 7a. The emission intensity at the pol β maximum at 343 nm in the complex with CPM-labeled dsDNA oligomer is decreased by ∼19%, compared to the free protein. Because CPM does not contribute to the tryptophan emission band at 343 nm, we can normalize the spectrum of the polymerase at 343 nm to the protein fluorescence intensity in the complex (Figure 7a). The difference between the normalized spectrum of the enzyme and the spectrum of the complex provides the sensitized emission spectrum of the labeled DNA with the maximum at ∼400 nm included in Figure 7a (*23*, *25*). The data indicate that in the presence of the donor (tryptophan residue of rat pol β) the fluorescence intensity of CPM at the 5′ end of the bound dsDNA 10-mer is increased by ∼30%. Analogous experiments have been performed with all DNA substrates and are shown in Figure 7b (substrate B), Figure 7c (substrate C), and Figure 7d (substrate D). Clearly, the spectral properties of all substrates are very similar and independent of the location of the acceptor on the DNA oligomer.

The apparent energy transfer efficiencies, E_D and E_A, and the true Förster transfer efficiency, E, of the examined substrates have been obtained using eqs 1, 3, and 4 and are included in Table 3. Although the apparent energy transfer efficiencies, E_D, would suggest the existence of some fluorescence energy transfer process, the value of E_A is practically zero providing $E = 0$ (eq 4), independent of the location of the acceptor. In other words, the observed changes in the donor and acceptor fluorescence spectra (Figure 7) result from the nondipolar emission changes induced by the complex formation but not from the energy transfer. Very little, if any, energy transfer from the tryptophan residue to the acceptor indicates that the bound nucleic acid is at a distance, from the tryptophan located on the 31-kDa domain, that is at least twice as large as the Förster critical distance of $R_0 = 21.6$ Å for the tryptophan and CPM pair (see Discussion).

The lack of any fluorescence energy transfer, observed with four different DNA substrates having different locations

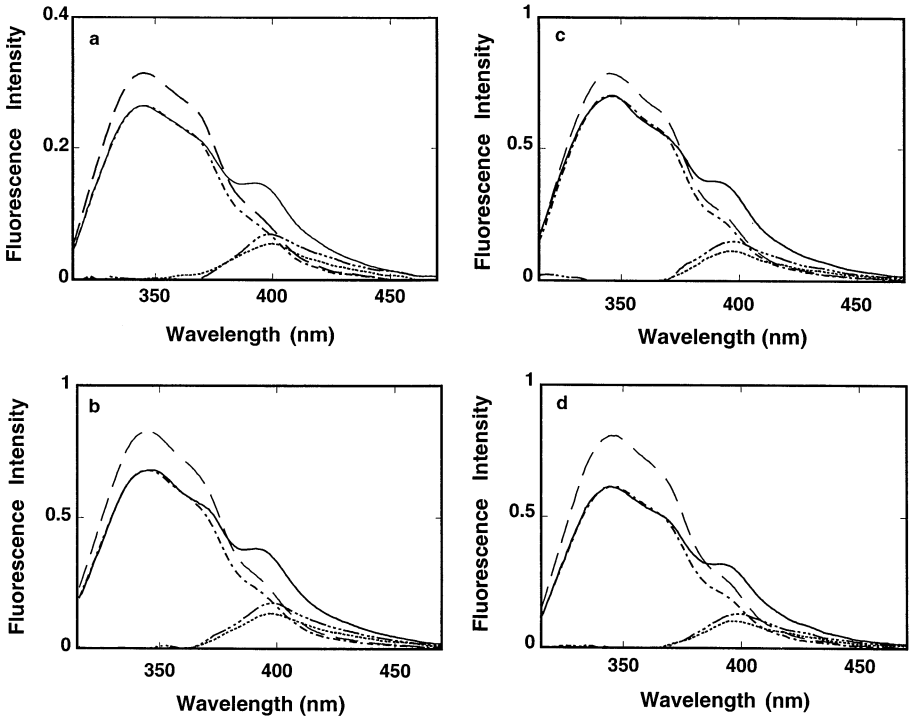

FIGURE 7: (a) Fluorescence emission spectrum of rat pol β alone (− −), the pol β−dsDNA oligomer complex (−), and the 5′-CPM-dsDNA oligomer (- - -) (Figure 1b, substrate A) (λ_{ex} = 295 nm) in buffer C (pH 7.0, 10 °C) containing 40 mM NaCl: the normalized emission spectrum of the polymerase to the maximum of the protein emission at 343 nm in the complex with the nucleic acid (− - −); the sensitized emission of the 5′-CPM-dsDNA oligomer in the complex with the polymerase (− - - -). (b) Fluorescence emission spectrum of rat pol β alone (− −), the pol β−5′-CPM-dsDNA oligomer complex (−), and the 5′-CPM-dsDNA oligomer (- - -) (Figure 1b, substrate B) (λ_{ex} = 295 nm) in buffer C (pH 7.0, 10 °C) containing 40 mM NaCl: the normalized spectrum of the polymerase to the maximum of the protein emission at 343 nm in the complex with the nucleic acid (− - −); the black line is the sensitized emission of the 5′-CPM-dsDNA oligomer in the complex with the polymerase (− - - -). (c) Fluorescence emission spectrum of rat pol β alone (− −), the pol β−3′-CPM-dsDNA oligomer complex (−), and the 3′-CPM-dsDNA oligomer (- - -) (Figure 1b, substrate C) (λ_{ex} = 295 nm) in buffer C (pH 7.0, 10 °C) containing 40 mM NaCl: the normalized spectrum of the polymerase to the maximum of the protein emission at 343 nm in the complex with the nucleic acid (− - −); the sensitized emission of the 3′-CPM-dsDNA oligomer in the complex with the polymerase (− - - -). (d) Fluorescence emission spectrum of rat pol β alone (− −), the pol β−3′-CPM-dsDNA oligomer complex (−), and the 3′-CPM-dsDNA oligomer (- - -) (Figure 1b, substrate D) (λ_{ex} = 295 nm) in buffer C (pH 7.0, 10 °C) containing 40 mM NaCl: the normalized spectrum of the polymerase to the maximum of the protein emission at 343 nm in the complex with the nucleic acid (− - −); the sensitized emission of the 3′-CPM-dsDNA oligomer in the complex with the polymerase (− - - -). Concentrations of pol β and the oligomer in all data presented in panels a−d are 3×10^{-7} and 5×10^{-7} M, respectively.

Table 3: Fluorescence Energy Transfer Parameters for Rat Pol β Complexes with the dsDNA 10-mer Containing CPM Residues at the 5′ or 3′ End (Figure 1b, Substrates A−D) in Buffer C (pH 7.0, 10 °C) Containing 40 mM NaCl

oligomer (Figure 1b)	J (M^{-1} cm^3)	r_{limN}	r_{limP}	E_D	E_A	E	R_0 (Å)	R (Å)
A (5′-CPM)	2.39×10^{-13}	0.18 ± 0.03	0.17 ± 0.05	0.32 ± 0.01	0 ± 0.005	0 ± 0.005	21.6	>55
B (5′-CPM)	2.39×10^{-13}	0.19 ± 0.03	0.17 ± 0.05	0.33 ± 0.01	0 ± 0.005	0 ± 0.005	21.6	>55
C (3′-CPM)	2.39×10^{-13}	0.17 ± 0.03	0.17 ± 0.05	0.44 ± 0.01	0 ± 0.005	0 ± 0.005	21.6	>55
D (3′-CPM)	2.39×10^{-13}	0.18 ± 0.03	0.17 ± 0.05	0.28 ± 0.01	0 ± 0.005	0 ± 0.005	21.6	>55

and environments around the acceptor, effectively excludes the possibility that the observed value of Förster energy transfer efficiency, E, is a consequence of a very peculiar orientation of the donor and acceptor, and/or their complete immobilization, that would result in $\kappa^2 = 0$ or 4 (*27*, *32*). Nevertheless, we have determined the limiting anisotropies of the pol β tryptophan and CPM located on the bound DNA oligomers (i.e., by eliminating the depolarization due to the macromolecular rotational movement) to assess mobilities of the donor and acceptor on the time scale of their fluorescence lifetimes. This approach is equivalent to the Perrin plot analysis at intermediate values of viscosity where macromolecular rotation is prevailing, without changing the temperature or introducing any additional solute to change the viscosity of the sample (*45*). The limiting anisotropy values for all examined DNA substrates are included in Table 3. The values are lower than the fundamental anisotropies of the tryptophan (∼0.27) (*46*), and particularly CPM (∼0.38) (Bujalowski, unpublished data), at the selected excitation wavelengths, indicating that the donor and the acceptor possess significant rotational mobility on the time scale of their fluorescence lifetimes. These data provide additional information indicating that E is not significantly affected by any peculiar orientation and immobilization of the donor and acceptor.

DISCUSSION

Site-Size of the Rat Pol β−dsDNA Complex Is 5 ± 1 Base Pairs, Indicating the Involvement of Only One of the Two DNA-Binding Subsites of the Enzyme in Interactions with

the dsDNA. Studies described in this work provide, for the first time, a direct insight into the complex energetics and structure of rat pol β interactions with the dsDNA. The site-size of a protein−DNA complex corresponds to the number of nucleotide residues, or base pairs, occluded by the protein (*33*, *39*, *40*, *41*). This fundamental quantity, characterizing a protein−nucleic acid complex, has a profound importance for any quantitative analysis of the functioning of an enzyme (*39*, *40*). A striking feature of the rat pol β−dsDNA complex is the small site-size, $n = 5 \pm 1$ base pairs, of the complex. Recall that the total DNA-binding site of pol β is built of two DNA-binding subsites each located on a different structural domain of the enzyme (Figure 6). Each DNA-binding subsite, one located on the 8-kDa domain and the other one on the 31-kDa domain, can bind nucleic acid by engaging ~5−10 base pairs (*12*−*15*). When the total DNA-binding site is engaged in interactions with the ssDNA, forming the $(\text{pol } \beta)_{16}$ binding mode, it encompasses 16 ± 2 nucleotide residues; i.e., both DNA-binding subsites of the polymerase are engaged in the interactions with the ssDNA (*12*−*15*). The determined site-size of the polymerase−dsDNA complex is much smaller than the site-size of the $(\text{pol } \beta)_{16}$ binding mode. Thus, the thermodynamic data show that the enzyme binds the dsDNA using only one of the DNA-binding subsites in the formed complexes, resulting in a site-size of about five base pairs occluded by the protein. As we pointed out, the independence of the rat pol β−dsDNA stoichiometry upon the DNA oligomer concentration indicates that one of the DNA-binding subsites is not capable of engaging in interactions with the dsDNA once the DNA oligomer is already bound to the enzyme (Figure 2a).

Rat Pol β Binds the dsDNA Using Exclusively Its 8-kDa Domain. The small site-size of the rat pol β−dsDNA complex is not without precedence. It is analogous to the formation of the $(\text{pol } \beta)_5$ binding mode observed in the complexes of rat and human pol β with the ssDNA (*12*−*15*). The site-size of the enzyme−dsDNA complex is $n = 5 \pm 1$ base pairs, the same as $n \approx 5$ that has been determined for the $(\text{pol } \beta)_5$ binding mode, where only the 8-kDa domain of the enzyme engages in the interactions with the nucleic acid. Moreover, when the ssDNA oligomer bound to the 8-kDa domain is too short to form the $(\text{pol } \beta)_{16}$ binding mode, the DNA-binding subsite located on the 31-kDa domain is not capable of accepting another oligomer mainly because of its low affinity (*12*). This is exactly what is observed in the binding of the dsDNA 10-mer to the polymerase (Figure 2). Furthermore, although only a single DNA-binding subsite is involved in interactions with the nucleic acid, the polymerase still has a high intrinsic affinity for the DNA. Such strong intrinsic affinity for the ss as well as dsDNA conformation is available to the enzyme only at the DNA-binding subsite located on the 8-kDa domain (*12*−*16*). Therefore, the obtained thermodynamic data provide first evidence that, in the binding to the dsDNA, rat pol β engages exclusively the 8-kDa domain in the interactions with the nucleic acid.

The results and discussion above, indicating that the rat pol β binds the dsDNA using only its 8-kDa domain, are directly supported by the fluorescence energy transfer data using four DNA oligomers with the fluorescence acceptor placed at the 5′ or 3′ end of the nucleic acid (Figure 1b). Independent of the acceptor location, the fluorescence energy transfer efficiency E is 0, indicating that the entire DNA molecule is separated from the single tryptophan located on the 31-kDa domain by a distance that is much larger than the Förster critical distance of the considered donor−acceptor pair, $R_0 = 21.6$ Å. One can estimate the minimum distance that would result in $E \approx 0$, using the relationship between E and R obtained by rearranging eq 5 to give

$$E = \frac{1}{1 + \left(\frac{R}{R_0}\right)^6} \tag{16}$$

It is clear that for the value of E to be ~0, with $R_0 = 21.6$ Å, R has to be at least 55 Å.

Such a large value of R is incompatible with the dsDNA oligomer bound to the 31-kDa domain. Average distances between the specific locations on the bound dsDNA oligomer and the tryptophan residue, W325, on the 31-kDa domain can be estimated using enzyme models based on its crystal structure. Figure 8a shows the hypothetical complex of pol β in "open" conformation with the dsDNA 10-mer placed

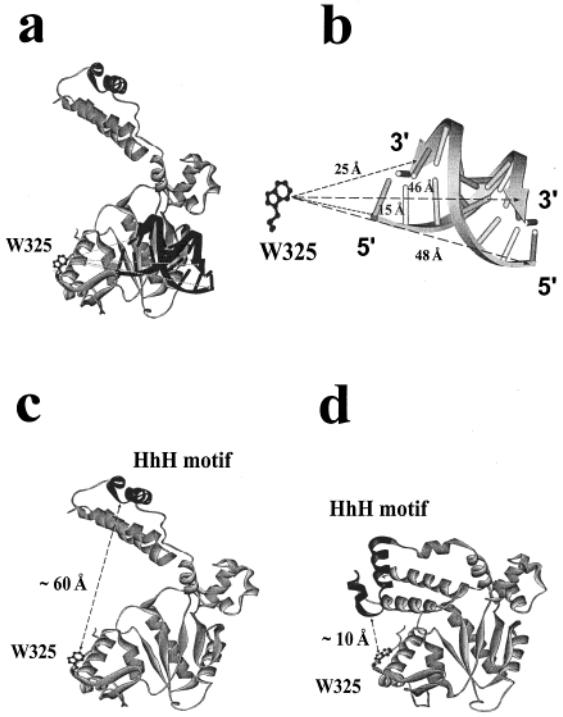

FIGURE 8: (a) Hypothetical structure of the mammalian pol β−dsDNA 10-mer complex if the nucleic acid were bound to the 31-kDa domain of the protein. The protein is in the "open" conformation and its structure has been generated using data from Brookhaven Protein Data Bank, under the codes 1BPD (protein) and 1BPY (nucleic acid), using ViewerPro (San Diego, CA). (b) Distances (Å) between the single tryptophan residue, W325, on the 31-kDa domain of the polymerase and the 5′ and 3′ ends of the bound dsDNA 10-mer, are extracted from Figure 8a, if the oligomer were bound to the 31-kDa domain (see text for details). (c) Location of the single tryptophan residue, W325, in the three-dimensional structure of pol β together with the distance (Å) between the tryptophan residue and the HhH DNA-binding motif (dark area) in "open" conformation of the enzyme (*47*). (d) Distance (Å) between the tryptophan residue, W325, and the HhH DNA-binding motif on the 8-kDa domain of pol β in "closed" conformations of the enzyme. The protein structures have been generated using data from Brookhaven Protein Data Bank, under codes 1BPD and 1BPY, respectively, using ViewerPro (San Diego, CA).

in the DNA-binding subsite on the 31-kDa domain. The dsDNA is modeled in A-DNA conformation as indicated by the crystallographic data. Note that because pol β does not have a preference for the sequence of the nucleic acid, the dsDNA 10-mer can, in general, be bound in two different orientations to the binding site. However, placement of a single acceptor at all four possible end locations of the nucleic acid eliminates any possible bias resulting from the DNA orientation. Fluorescence energy transfer measurements provide information about the distance between the donor and acceptor averaged over all possible orientations.

Figure 8b shows the extracted distances from the tryptophan residue, W325, on the 31-kDa domain to the examined locations of the acceptor on the bound dsDNA 10-mer if the oligomer were bound to the 31-kDa domain. The estimated distances to the 5′ ends of the nucleic acid are 15 ± 3.5 and 46 ± 3.5 Å, respectively, with the average R being 30.5 ± 3 Å. The included large errors take into account that the average location of the label can be, at most, equivalent to an additional base at the end of the DNA. The same distances to the 3′ ends are 25 ± 3.5 and 48 ± 3.5 Å, and the average R is 36.5 ± 3 Å. Using eq 16 and R_0 = 21.6 Å, one can estimate the value of E that should be observed if the dsDNA 10-mer were bound to the 31-kDa domain. The obtained values of E are 0.12 ± 0.05 and 0.05 ± 0.02 for the 5′ ends and 3′ ends, respectively. They are dramatically larger than the $E = 0$ experimentally observed, even with the included large errors (Table 3).

The situation is very different with the DNA-binding subsite located on the 8-kDa domain. The location of the bound dsDNA oligomer on the 8-kDa domain can only be inferred from the crystal structure of the enzyme cocomplexes with the gapped DNA (*7*). The domain contains the helix−hairpin−helix motif (HhH), a nonspecific DNA-binding motif (*47*). The HhH motif has been proposed as the central part of the DNA binding subsite in the polymerase−gapped DNA complexes (*7*). In the open conformation of the enzyme (Figure 8c), the distance from the HhH motif to the single tryptophan, W325, on the 31-kDa domain is ∼60 Å. Distances between the 5′ or 3′ ends of the bound dsDNA oligomer and the tryptophan residue will be even larger. Thus, with the dsDNA 10-mer placed at this minimum distance, there will not be any detectable fluorescence energy transfer from the acceptor on the nucleic acid and from the protein tryptophan on the 31-kDa domain, in excellent agreement with the experimentally observed value of E = 0.

Pol β Binds dsDNA in an Open Conformation. It should be pointed out that the distance from the HhH motif on the 8-kDa domain to the tryptophan residue, W325, on the 31-kDa domain has been estimated using the open conformation of the enzyme (Figure 8c). When the enzyme is bound to the gapped DNA substrates, it assumes a "closed" conformation as a result of the engagement of the 31-kDa domain in interactions with the nucleic acid, depicted in Figure 8d. In closed conformation, the distance between the HhH motif and the single tryptophan residue is reduced to ∼10 Å. Such a conformational change does not affect the distances between the single tryptophan and the DNA-binding subsite on the 31-kDa domain because they are located on the same domain. However, if pol β were in the closed conformation with the dsDNA oligomer bound at the 8-kDa domain, then the fluorescence energy transfer efficiencies would not be zero but about 0.3−1 (eq 16), very easy to detect and dramatically larger than the experimentally observed E = 0. Therefore, the lack of any experimentally detectable fluorescence energy transfer can only be explained if the polymerase binds the dsDNA using exclusively its 8-kDa domain and the enzyme is in "open" conformation in the complex with the dsDNA.

Salt Effect on the Intrinsic Affinity of the Rat Pol β−dsDNA Complex Is Dominated by Cation Release. Additional evidence for the proposed involvement of the 8-kDa domain DNA-binding site in interactions with the dsDNA comes from the salt effect on the observed intrinsic affinity of the rat pol β−dsDNA complex. The data obtained in the absence of magnesium are of particular importance because complications resulting from the presence of the additional Mg^{2+} ligand are not present (see below). Crystallographic data indicate that in the cocomplex the 8-kDa domain engages in interactions only with one strand of the dsDNA (*7*). In this context, the slopes $\partial \log K/\partial \log [NaCl] = -4 \pm 0.5$ and $\partial \log K/\partial \log [NaBr] = -5.3 \pm 0.5$ obtained for the intact enzyme−dsDNA complex are similar, although not identical, to the slopes $\partial \log K/\partial \log [NaCl] = -4.8 \pm 0.5$ and $\partial \log K/\partial \log [NaBr] = -4.5 \pm 0.5$ obtained for the salt dependence of the intrinsic affinity of the isolated 8-kDa domain−ssDNA complex upon salt concentration (*42*−*44*). Bromide anions, Br^-, are known to have significantly higher affinity for protein amine groups than Cl^- (*48*). In the case of the isolated 8-kDa domain, the lack of a significant difference between the slopes obtained in the presence of NaCl and NaBr indicated that the net ion release includes only cations and that interactions are dominated by electrostatic components of the free energy of binding (*16*). A higher value of the net number of ions released observed for the intact enzyme in the presence of NaBr indicates that additional anions are released from the intact pol β when chloride is replaced by bromide. Nevertheless, similar to the isolated 8-kDa domain, the obtained values of the net ion releases in the presence of NaCl and NaBr indicate that the net ion release accompanying intrinsic interactions of the intact enzyme with the dsDNA is still dominated by the cations (*42*, *43*). This is an expected result for the dominant involvement of the DNA-binding subsite located on the 8-kDa domain in interactions with dsDNA, which forms multiple ionic contacts with the nucleic acid (*16*).

Salt Effect on Cooperative Interactions Indicates Direct Protein−Protein Interactions in the Complex with the dsDNA. A peculiar aspect of the rat pol β binding to the dsDNA is the presence of significant cooperative interactions. Moreover, the salt effect on the cooperative interactions is dramatically different from the analogous effect on the intrinsic affinity. First, in the absence of Mg^{2+}, the positive slopes $\partial \log \omega/\partial \log [NaCl] = 2.8 \pm 0.4$ and $\partial \log \omega/\partial \log [NaBr] = 4.5 \pm 0.5$ show that a net ion uptake accompanies cooperative interactions. Thus, although the intrinsic affinity decreases, positive cooperative interactions strongly increase with the increasing salt concentration (see below). Second, there is a large difference between the net number of ion uptakes observed in the presence of Cl^- and Br^-, an indication that a significant net uptake of anions occurs in the formation of cooperative contacts. Because the negatively charged DNA does not bind anions, the large

contribution of anions to the net ion uptake provides evidence that the cooperative interactions result from direct protein−protein interactions between the bound pol β molecules.

The observed salt effect on cooperative interactions between pol β molecules bound to the dsDNA is very different from the salt effect on weak cooperative interactions between bound enzyme molecules in the (pol β)$_5$ binding mode on the ssDNA and gapped DNA, where no dependence or little dependence upon salt has been found (*12*, *14*, *15*). In other words, only cooperative interactions between protein molecules bound to the dsDNA and not the ssDNA are significantly controlled by the salt concentration. Note that this control is dramatic. While at higher salt concentration ω is large, indicating strong attractive interactions between the bound proteins. At low salt concentration, $\leq$50 mM, ω is much lower than 1, indicating strong repulsive interactions. Such a large difference in the thermodynamic response of enzyme complexes with the dsDNA versus the complexes with the ssDNA and gapped DNA to the salt concentration in solution indicates that very different interacting areas of the protein are involved in cooperative interactions. Thus, these results indicate that the orientation of the polymerase bound to the dsDNA is very different from the orientation of the enzyme bound to the ssDNA or gapped DNA substrates (*12*, *14*, *15*). These changes in the enzyme orientation in complexes with different DNA conformations may play an important role in the damaged DNA recognition (see below).

Anion Release Accompanying the Intrinsic dsDNA Binding and Cooperative Interactions in the Presence of Magnesium Indicates Direct Mg^{2+} Binding to the Enzyme. A profound role of magnesium in affecting interactions of the isolated 8-kDa domain with the ssDNA has been described by us before (*16*). The site-size of the 8-kDa domain complex with the ssDNA is reduced from 13 $\pm$ 0.7 to 9 $\pm$ 0.6 nucleotide residues. Moreover, magnesium affects the anion release from the domain. The effect is completely saturated at the [$MgCl_2$] of ~1 mM; thus, magnesium binding sites participating in the process must be characterized by the binding constant $\geq 10^4$ M^{-1}. The high affinity indicates that in examined solution conditions, [NaCl] > 0.1 M, the decrease of the site-size is induced by Mg^{2+} binding to the domain and not to the ssDNA (*42*, *43*).

Direct Mg^{2+} binding to the polymerase is also evident from the observed changes in the net ion release and uptake accompanying intrinsic and cooperative interactions in the rat pol β−dsDNA complex formation in the presence of $MgCl_2$. Magnesium increases the net ion release in the intrinsic binding of the enzyme to the dsDNA in the presence of Cl^- and only slightly decreases the ion release in the presence of Br^- (Figures 4 and 5). This is a surprising result. A rather strong decrease of the net number of ions released is always expected due to the competition between Mg^{2+} and Na^+ for the DNA (*42*−*43*). These data indicate that Mg^{2+} binding to the enzyme affects the anion association with the polymerase, as previously observed for the isolated 8-kDa domain−ssDNA complex (*16*).

In the case of cooperative interactions, Mg^{2+} strongly increases the net ion uptake observed in the presence of Cl^-, with the slope $\partial \log \omega / \partial \log [NaCl] = 4.5 \pm 0.5$ as compared to $\partial \log \omega / \partial \log [NaCl] = 2.8 \pm 0.4$, obtained in the absence of Mg^{2+}. Analogous slopes, obtained in the presence of NaBr, are $\partial \log \omega / \partial \log [NaBr] = 3.5 \pm 0.4 \pm 0.5$ and $\partial \log \omega / \partial \log [NaBr] = 4.5 \pm 0.5$, indicating that magnesium decreases the ion uptake by the complex (Figures 4 and 5). The difference between the magnesium effects in the presence of different anions suggests that rat pol β has multiple anion binding sites that gain preference for chloride anions, as compared to Br^-, in the presence of Mg^{2+}. We cannot exclude that the magnesium form of the enzyme has an increased number of anion binding sites, although that would lead to the same effect on ion release, independent of the type of anion. Therefore, we favor an interpretation that magnesium binding does not change the number of the anion binding sites but increases their affinity and specificity for Cl^-, leading to an increased number of Cl^- anions bound. Moreover, the observed effect of Mg^{2+} on cooperative interactions between the polymerase molecules bound to the dsDNA provides evidence that the effect of magnesium predominantly results from the polymerase conformational changes induced by specific Mg^{2+} cations binding to the enzyme.

Why Is Rat Pol β Not Forming Different Binding Modes with the dsDNA? Recent kinetic studies of the human and rat pol β binding to the ssDNA and gapped DNA substrates clearly showed that the enzymes initiate binding to the nucleic acid using the DNA-binding subsite on the 8-kDa domain (*18*−*20*). In fact, the enzyme is bound to the nucleic acid exclusively through the 8-kDa domain in the first intermediate. This is true for both the (pol β)$_{16}$ and (pol β)$_5$ binding modes as well as for the gap complex formation. In other words, the 8-kDa domain is the DNA binding initiation domain, independent of the conformation of the nucleic acid. The enzyme achieves the free access of the nucleic acid to the 8-kDa domain by maintaining the open conformation in solution and in the first intermediate. The structure of the DNA-binding subsite on the 8-kDa domain allows the enzyme to engage only a part of the subsite in interactions with the nucleic acid and to impose a specific conformation and orientation of the bound enzyme with respect to the DNA that depends on the structure of the nucleic acid (*16*). As discussed above, the orientation of the bound polymerase is different in the complexes with the ssDNA or gapped DNA substrates as reflected by the very different effects of the enzyme on the nucleic acid structure in different complexes and cooperative interactions between bound polymerase molecules (*12*−*15*).

Recall that only after engagement of the 8-kDa domain in interactions with the nucleic acid may the 31-kDa domain associate with the nucleic acid, inducing global conformational changes in the DNA and docking the enzyme on the nucleic acid (*18*−*20*). In the case of the ssDNA and gapped DNA substrates, this association process results in formation of the (pol β)$_{16}$ binding mode or gap complex (*12*−*15*). However, the efficiency of this process depends on the enzyme orientation, imposed by the 8-kDa domain, and the structure of the DNA. With flexible structures such as that of the ssDNA and gapped DNA, conformational changes of the nucleic acid can be easily induced and the enzyme orientation in the complex is unfavorable for strong cooperative interactions. Therefore, the association process of the 31-kDa domain with the nucleic acid is very efficient, leading to the formation of the (pol β)$_{16}$ binding mode or gap complex. With the dsDNA, the situation is different. The

structure of the nucleic acid is very stiff, allowing only limited global structural changes of the nucleic acid, and the orientation of the enzyme favors strong positive cooperative interactions. As a result of these two factors, the bound enzyme predominantly remains in the open conformation, associated with the nucleic acid through its 8-kDa domain, in the complex stabilized by strong positive cooperative interactions.

Functional Implications of the Cooperative Binding of Rat Pol β to the dsDNA. The results obtained in this work indicate that the intrinsic binding constant, K, and cooperative interaction parameter, ω, obtained for the polymerase binding to the dsDNA are significantly higher than the corresponding parameters for the enzyme binding to the ssDNA conformation in the (pol β)$_5$ binding mode determined previously, in the same solution conditions, with the ssDNA polymers and oligomers (*12*, *13*). For instance, in the presence of 100 mM NaCl and 1 mM $MgCl_2$, $K = 4.4 \times 10^5$ M^{-1} and $\omega = 35 \pm 7$ with the dsDNA, as compared to $K = (1.2 \pm 0.5) \times 10^4$ M^{-1} and $\omega = 6 \pm 3$, obtained for the (pol β)$_5$ binding mode (*12*). Moreover, although intrinsic affinities on both the ss and dsDNA decrease with increasing salt concentration, only cooperative interactions between bound pol β molecules to the dsDNA strongly increase with the increased salt concentration. In the presence of magnesium, ω reaches a value of ~150 at 150 mM NaCl (Table 2). In other words, the increased cooperative interactions compensate for the diminished intrinsic affinity for the dsDNA at higher salt concentrations. This is very different from the interactions with the ssDNA where cooperative interactions are weak and little salt-dependent (*12*). As a result, rat pol β will preferentially bind to the dsDNA conformation over the ssDNA mostly because of the amplifying effect of cooperative interactions between bound enzyme molecules.

This behavior excludes the possibility that the enzyme intrinsic affinity for the ssDNA alone plays a significant role in the recognition of the gapped DNA by the polymerase, as previously deemed when the energetics of the enzyme binding to the dsDNA and the topology of the complex were not yet known (*12*−*15*). Recall that the intrinsic affinity of the gap complex is significantly higher than the intrinsic affinity for the dsDNA, determined in this work (*14*, *15*). However, this is only because of the engagement of both DNA-binding subsites in interactions with the DNA in the gap complex. On the other hand, in the case of a large excess of the dsDNA, with a large number of potential binding sites and strong positive cooperative interactions, the difference between the intrinsic affinities for the dsDNA versus gapped DNA may not be high enough to provide the required selectivity for the damaged DNA. Thus, the remaining question is the following. What is the possible role of the discovered strong cooperative interactions in the pol β−dsDNA association in the recognition of the gapped DNA in the context of overwhelming dsDNA conformation?

Kinetic studies of rat and human pol β interactions with gapped DNAs indicate that in this first binding step only the 8-kDa domain of the enzyme engages in interactions with the nucleic acid (*18*−*20*). The process is very fast, leading to rapid release of the polymerase from the complex, if the orientation of the enzyme does not lead to the fast engagement of the 31-kDa domain in the complex. In small patches of the dsDNA, resulting in limited trial and error associations, this mechanism could be sufficient for selectivity (*18*, *19*). However, in a large excess of the dsDNA, the recognition of the specific damaged DNA structure would be an inefficient process that would require multiple association and dissociation steps to examine the DNA substrates, particularly at a high salt concentration in the vicinity of the dsDNA.

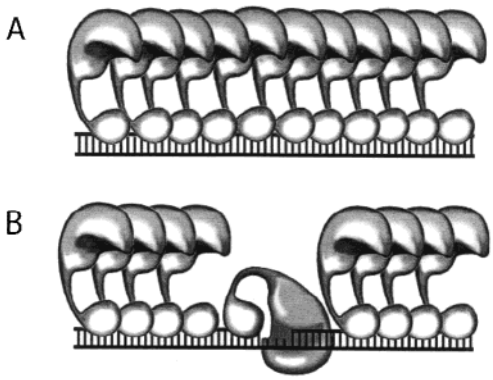

FIGURE 9: Schematic model of the role of the positive cooperativity in the gapped DNA recognition by mammalian pol β. Binding of the enzyme to the dsDNA is characterized by strong positive cooperative interactions resulting in the formation of protein clusters on the nucleic acid lattice (A). The cooperative interactions prevent the dissociation of enzyme from the DNA. From encounters with the ssDNA conformation of the gap, the cooperative interactions with the protein cluster on the dsDNA become weak because of the lower ion concentration and changed orientation of the polymerase resulting from the engagements of the 31-kDa domain in the complex with the nucleic acid. The 31-kDa domain association process is also facilitated by the higher flexibility of the ssDNA of the gap (B). The polymerase breaks its ties with the protein cluster and forms the gap complex capable of catalysis.

A plausible model of the possible role of cooperative binding to the dsDNA in recognition of a damaged gapped DNA in the presence of the excess dsDNA, based on the results described in this work, is schematically depicted in Figure 9. The enzyme cooperatively binds to the dsDNA, using exclusively the 8-kDa domain and with the site-size of $n = 5$ base pairs. In this complex the polymerase does not engage the catalytic site on the 31-kDa domain in interactions with the nucleic acid (Figure 9a). On the other hand, cooperative interactions will prevent the enzyme from dissociating from the nucleic acid. Instead of a single complex, a protein cluster is formed that allows the enzyme to examine longer patches of the dsDNA. This takes place only until the damaged DNA, the ssDNA gap, is encountered.

As discussed above, strong cooperative interactions result from a specific orientation of the enzyme bound to the dsDNA that favors protein−protein interactions. On the other hand, previous studies of the human and rat pol β binding to the gapped DNA clearly indicated that both enzymes assume a very different and specific orientation and/or conformation when bound in a gap complex in which both the 8- and 31-kDa domains are engaged in the complex with the nucleic acid (*14*, *15*, *20*). This is particularly true in the presence of the 5′ terminal phosphate group downstream from the primer, a common product in the base excision repair (*6*, *14*, *15*). Note also that the concentration of ions around ssDNA of the gap is lower than around the dsDNA conformation as a result of the lower charge density of the ssDNA (*42*, *44*, *49*). Moreover, the ssDNA conformation is

much more flexible than the dsDNA. In this different orientation or conformation in the gap complex and at lower ion concentration, cooperative interactions with the remaining pol β molecules bound to the dsDNA become very weak, if any, as experimentally determined (*14*, *15*). In other words, the polymerase molecule, encountering the gap, breaks its ties with the protein cluster on the dsDNA and forms a gap complex (Figure 9b). The induced conformational transitions may also extend into the catalysis (*50*). The enzyme, now free from interactions with the remaining polymerase molecules bound to the dsDNA, engages the 31-kDa domain in interactions with the nucleic acid and may initiate catalytic steps.

ACKNOWLEDGMENT

We thank Mrs. Betty Sordahl for her help in preparing the manuscript.

REFERENCES

1. Friedberg, E. C., Walker, G. C., and Siede, W. (1995) *DNA Repair and Mutagenesis*, pp 317−365, ASM Press, Washington, DC.
2. Kornberg, A., and Baker, T. A. (1992) *DNA Replication*, pp 197−225, W. H. Freeman, New York.
3. Budd, M. E., and Campbell, J. L. (1997) *Mutat. Res. 384*, 157−167.
4. Fry, M., and Loeb, L. A. (1986) *Animal Cell DNA Polymerases*, pp 75−183, CRC Press, Inc., Boca Raton, FL.
5. Hubscher, U., Nasheuer, H.-P., and Syvaoja, J. E. (2000) *Trends Biochem. Sci. 25*, 143−147.
6. Masumoto, Y., and Kim, K. (1995) *Science 269*, 699−702.
7. Pelletier, H., Sawaya, M. R., Wolfle, W., Wilson, S. H., and Kraut, J., (1996) *Biochemistry 35*, 12762−12777.
8. Nagasawa, K.-I., Kitamura, K., Yasui, A., Nimura, Y., Ikeda, K., Hirai, M., Matsukage, A., and Nakanishi, M. (2000) *J. Biol. Chem. 275*, 31233−31238.
9. Dominguez, O., Ruiz, J. F., Lain de Lera, T., Garcia-Diaz, M., Gonzalez, M. A., Kirchhoff, T., Martinez, A. C., Bernad, A., and Blanco, L. (2000) *EMBO J. 19*, 1731−1742.
10. Garcia-Diaz, M., Dominguez, O., Lopez-Fernandez, L. A., Lain de Lera, T., Saniger, M. L., Ruiz, J. F., Parraga, M., Gacia-Ortiz, M. J., Kirchhoff, T., del Mazo, J., Bernad, A., and Blanco, L. (2000) *J. Mol. Biol. 301*, 851−867.
11. Oliveros, M., Yanez, R. J., Salas, M. L., Vinuela, E., and Blanco, L. (1997) *J. Biol. Chem. 272*, 30899−30910.
12. Rajendran, S., Jezewska, M. J., and Bujalowski, W. (1998) *J. Biol. Chem. 273*, 31021−31031.
13. Jezewska, M. J., Rajendran, S., and Bujalowski, W. (1998) *J. Mol. Biol. 284*, 1113−1131.
14. Rajendran, S., Jezewska, M. J., and Bujalowski, W. (2001) *J. Mol. Biol. 308*, 477−500.
15. Jezewska, M. J., Rajendran, S., and Bujalowski, W. (2001) *J. Biol. Chem. 276*, 16123−16136.
16. Jezewska, M. J., Rajendran, S., and Bujalowski, W. (2001) *Biochemistry 40*, 3295−3307
17. Matsumoto, Y., Kim, K., Katz, D. S., and Feng, J.-A. (1998) *Biochemistry 37*, 6456−6464.
18. Jezewska, M. J., Rajendran, S., Galletto, R., and Bujalowski, W. (2001) *J. Mol. Biol. 313*, 977−1002.
19. Rajendran, S., Jezewska, M. J., and Bujalowski, W. (2001) *Biochemistry 40*, 11794−11810.
20. Jezewska, M. J., Galletto, R., and Bujalowski, W. (2002) *J. Biol. Chem. 277*, 20316−20327.
21. Edeldoch, H. (1967) *Biochemistry 6*, 1948−1954.
22. Gill, S. C., and von Hippel, P. H. (1989) *Anal. Biochem. 182*, 319−326.
23. Jezewska, M. J., Rajendran, S., and Bujalowski, W. (1998) *Biochemistry 37*, 3116−3136.
24. Jezewska, M. J., Rajendran S., and Bujalowski, W. (1998) *J. Biol. Chem. 273*, 9058−9069.
25. Jezewska, M. J., Rajendran, S., Bujalowska, D., and Bujalowski, W. (1998) *J. Biol. Chem. 273*, 10515−10529.
26. Azumi, T., and McGlynn, S. P. (1962) *J. Chem. Phys. 37*, 2413−2420.
27. Lakowicz, J. R. (1999) *Principle of Fluorescence Spectroscopy*, pp 367−443, Plenum Press, New York.
28. Parker, C. A., and Reese, W. T. (1960) *Analyst 85*, 587−592.
29. Parker, C. A. (1962) *Anal. Chem. 34*, 502−505.
30. Scott, T. G., Spencer, R. D., Leonard, N. J., and Weber, G. (1970) *J. Am. Chem. Soc. 92*, 687−695.
31. Berman, H. A., Yguerabide, J., and Taylor, P. (1980) *Biochemistry 19*, 2226−2235.
32. Dale, R. E., Esinger, J., and Blumberg, W. E. (1979) *Biophys. J. 26*, 161−194.
33. Lohman, T. M., and Bujalowski, W. (1991) *Methods Enzymol. 208*, 258−290.
34. Bujalowski, W., and Klonowska, M. M. (1993) *Biochemistry 32*, 5888−5900.
35. Jezewska, M. J., and Bujalowski, W. (1996) *Biochemistry 35*, 2117−2128.
36. Bujalowski, W., and Jezewska, M. J. (1995) *Biochemistry 34*, 8513−8519.
37. Bujalowski, W., and Jezewska, M. J. (2000) in *Spectrophotometry & Spectrofluorimetry. A Practical Approach* (Gore, M. G., Ed.), pp 141−165, Oxford University Press, Oxford, U.K.
38. Hill, T. L. (1985) *Cooperativity Theory in Biochemistry*, pp 167−234, Springer-Verlag, New York.
39. Epstein, I. R. (1978) *Biophys. Chem. 8*, 327−339.
40. McGhee, J. D., and von Hippel, P. H. (1974) *J. Mol. Biol. 86*, 469−489.
41. Bujalowski, W., Lohman, T. M., and Anderson, C. F. (1989) *Biopolymers 28*, 1637−1643.
42. Record, M. T., Jr., Anderson, C. F., and Lohman, T. M. (1978) *Q. Rev. Biophys. 11*, 103−178.
43. Record, M. T., Lohman, T. M., and deHaseth, P. L. (1976) *J. Mol. Biol. 107*, 145−158.
44. Olmsted, M. C., Bond, J. P., Anderson, C. F., and Record, M. T. (1995) *Biophys. J. 68*, 634−647.
45. Cantor, C. R., and Schimmel, P. R. (1980) *Biophysical Chemistry*, Part II, pp 433−466, W. H Freeman and Company, New York.
46. Eftink, M. R., Selvidge, L. A., Callis, P. R., and Rehms, A. A. (2000) *J. Phys. Chem. 94*, 3469−3479.
47. Doherty, A. J., Serpell, L. C., and Ponting, C. P. (1996) *Nucleic Acids Res. 24*, 2488−2497.
48. von Hippel, P. H., and Schleich T. (1969) in *Structure of Biological Macromolecules* (Timasheff, S., Fasman G. D., Eds.), pp 417−575, M. Dekker, New York.
49. Manning, G. (1978) *Q. Rev. Biophys. 11*, 103−178.
50. Zhong, X., Patel, S. S., Werneburg, B. G., and Tsai, M.-D. (1997) *Biochemistry 36*, 11891−11900.

BI030046F